DET NORSKE VIDENSKAPS-AKADEMI I OSLO

GEOFYSISKE PUBLIKASJONER
GEOPHYSICA NORVEGICA

Vol. XXIII. No. 1 January 1962

BERNT MÆHLUM

The sporadic *E* auroral zone

OSLO 1962
OSLO UNIVERSITY PRESS

GEOFYSISKE PUBLIKASJONER

GEOPHYSICA NORVEGICA

VOL. XXIII

UTGITT AV

DET NORSKE VIDENSKAPS-AKADEMI

I OSLO

OSLO 1962—63

UNIVERSITETSFORLAGET

GEOFYSISKE PUBLIKASJONER
GEOPHYSICA NORVEGICA
VOL. XXIII. NO. 1

THE SPORADIC E AURORAL ZONE

By Bernt Mæhlum

FREMLAGT I VITENSKAPS-AKADEMIETS MØTE DEN 10DE MARS 1961 AV HARANG

Summary. The occurrence of the night-time *Es* ionization in and near the visual auroral zone has been studied. The main part of the investigation is based on the routine $h'(f)$ records obtained during and after the IGY in Scandinavia. Special emphasis is placed on the relationship between the "sporadic *E* auroral zone" and the geomagnetic storm current system.

The "*large scale*" structure of the night-time *Es* layer near the auroral zone has been studied from simultaneous ionosoundings at three closely spaced recorders near Tromsø.

Possible sources of ionization for the different types of *Es* are discussed, and the paper closes with a discussion of the relationship between the ionization in the *Es*-zone and the conductivity in the storm current.

Introduction. The sporadic *E* layer in the ionosphere is known to undergo rapid and erratic variations. From statistical studies, some regular, latitude-dependent features have been deduced. It has therefore proved convenient to separate the northern hemisphere into four different «zones» of *Es* (Smith [1] and Coroniti and Penndorf [2]):

a) *Equatorial zone*
b) *Middle latitude zone*
c) *Auroral zone*
d) «*Thule type*» *zone*

The distinction between the zones is based upon statistical studies of *fEs* (*fEs* being the maximum frequency at which reflection from the *Es* layer is observed on the ionograms).

In the equatorial zone the observed *fEs* exceeds a selected limiting frequency of 5Mc sec^{-1} only during daytime, whereas such high values of *fEs* are mainly observed during the night in the auroral zone. At high latitudes (north of the auroral zone) and at middle latitudes *fEs* exceeds the limiting frequency practically only during the summer.

The transition regions between the different zones have not been much treated in the literature, and the meridional extent of the different zones is not well established. In fact, the dividing line between the different zones seems to be shifted in latitude, depending on the geophysical conditions. The meridional movements of the demarkation line between the middle latitude zone and the auroral zone are evident from the sporadic *E* observations at Lycksele, Sweden (64.6° N, 18.8° E, 62,7° geom lat). This

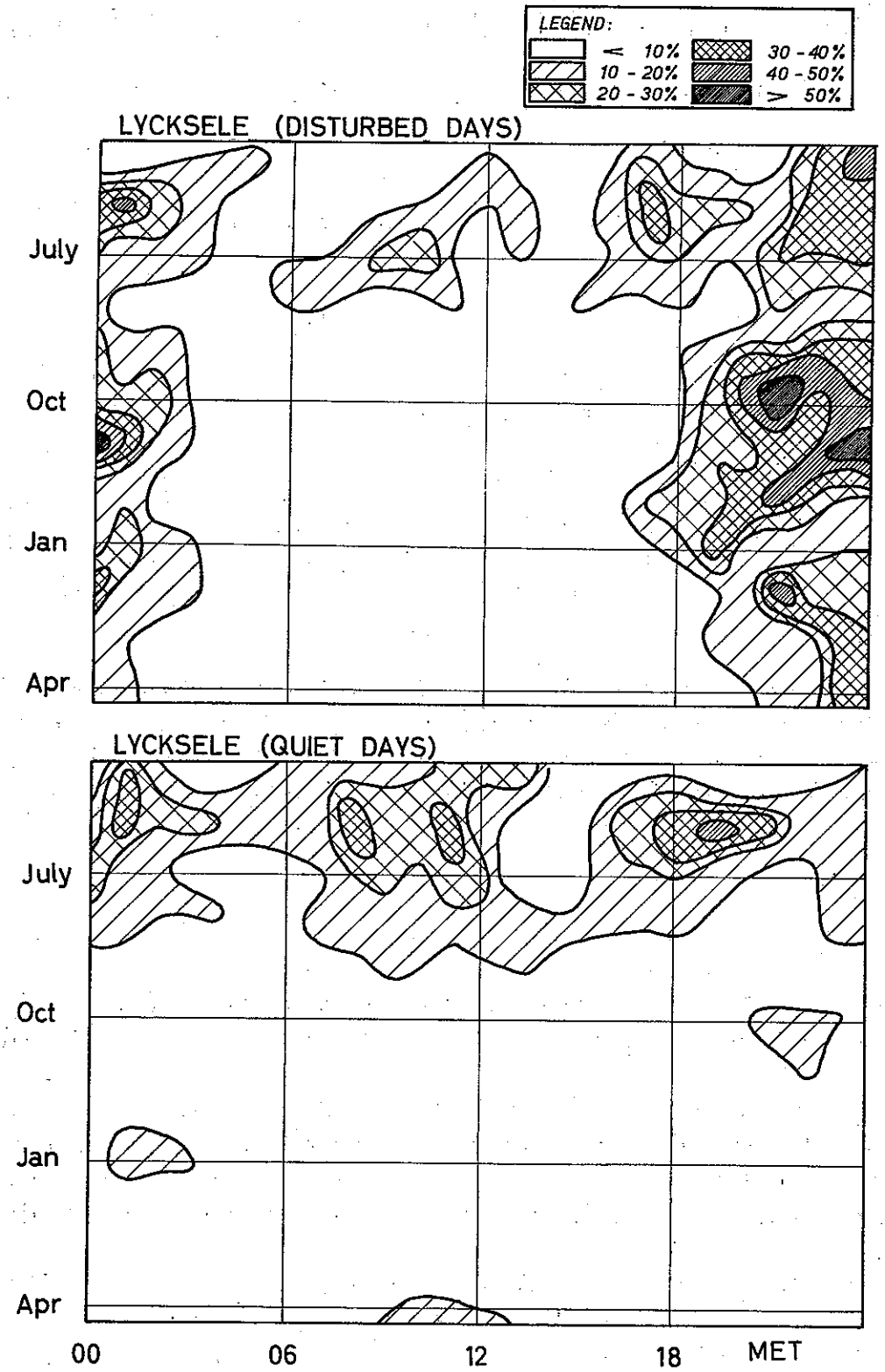

Fig. 1. Percentage occurrence of *fEs* exceeding 5 Mc sec^{-1} during (a) geomagnetically quiet conditions ($K \leqq 3$) and (b) during disturbed conditions ($K > 3$) (MÆHLUM [10]).

station is, according to the definition, a typical auroral zone *Es* station during geomagnetically disturbed conditions, whereas the station possesses the characteristics of a middle latitude station during quiet conditions (Fig. 1).

The present paper is mainly concerned with a study of (i) the regular and irregular variations of the night-time ionization of the sporadic *E* layer close to the visual auroral zone, and (ii) the relationship between the auroral zone of *Es* and the geomagnetic storm current. The study is based upon observations obtained at the Scandinavian stations given in Table 1, during the period 1957—60. Results from some ad hoc experiments are also included.

A brief survey of the present knowledge on the sporadic *E* ionization in the auroral zone is given in Section 2. Results from the study are presented in Sections 3—5. The paper is concluded with a discussion of the observational results.

As the planetary storm index may deviate appreciably from the local storm index in the auroral zone, especially during large polar storms, the local geomagnetic storm parameters from Tromsø have been used in the study.

Table 1. Routine ionosonde stations used in the study.

	Latitude	Longitude	Geom lat.
Longyearbyen	78,2° N	15,7° E	74
Tromsø	69,7° N	19,0° E	67
Kiruna	67,8° N	20,5° E	65
Lycksele	64,6° N	18,7° E	63
Kjeller	60,0° N	11,1° E	60
Upsala	59,8° N	17,6° E	59

2. Present knowledge. The sporadic *E* layer in the auroral zone has been studied by a large number of workers. (A survey of results has recently been given by SMITH and THOMAS [3]). In spite of this, not much is known about the temporal and spatial variations of the layer.

Two clearly distinguishable groups of *Es* traces are observed during the night in the auroral zone; the first one including all *Es* traces which show a clear group delay near the top frequency; the second one, with *Es* traces showing no group delay.

The retardation type of *Es* most probably refers to a thick, opaque layer in the *Es* region of the auroral ionosphere, with small semitransparent areas embedded (similar to Rawer's "*durchlöcherte Schicht*" model [4]). Normally the *fEs* is somewhat higher than the "*blanketing frequency*" (the lowest frequency at which the *F2* layer is observed). At times, however, the *F2* layer is completely obscured by the sporadic *E* layer at frequencies lower than *fEs*, and the *Es* layer may even produce a group delay in the *F2* trace near *fEs*. The *Es* layer which gives rise to a group delay in the *F2* trace is at some stations called "*night E*" and scaled as a normal *E* layer [6]. The retardation type

of *Es* is an auroral zone phenomenon exclusively, being rarely observed at middle latitudes (BECKER [5]).

The non-retardation types of *Es* traces observed during the night in the auroral zone are most probably due to partial reflections from thin layers of ionization or ledges in the electron density profile of the "background ionization". These types are normally transparent or semitransparent. The southern extent of the auroral, non-retardation types of *Es* is very uncertain, as *Es* traces which show no group retardation are regularly observed also at middle latitudes.

A third type of *Es* observed in the auroral zone is the so-called "*slant Es*". This type is due to off-zenithal reflections (OLESEN and RYBNER [8]), and will not be discussed in this paper.

The regular and irregular variation of *fEs* in the auroral zone has not been paid much attention in the literature. It has been shown (SMITH [1]) that the *fEs* exceeds the limiting frequency of 5 Mc sec^{-1} most frequently near local midnight. The diurnal maximum is found somewhat earlier at stations situated near the east coast of America (Narsassuak and Ft Chimo) than at stations further west (Fairbanks)[1]. The diurnal maximum seems to coincide with the maximum of geomagnetic activity (BESPROZVANNAYA and LOVCOVA [9]).

At sub-auroral zone stations there exists a clear positive correlation between the sporadic *E* ionization and magnetic activity [1]. For stations situated in and north of the visual auroral zone, however, the correlation is relatively poor. The correlation between the Tromsø *K*-index and the *fEs* as observed at the Scandinavian stations during night-time has been studied by the author [10]. The maximum correlation was found 4—5 degrees south of the visual auroral zone. At high latitudes (Longyearbyen) the correlation is negative.

The *Es* layer in the auroral zone is clearly associated with the occurrence of visual aurora. KNECHT [11] has shown that the *fEs*, as observed during the night at a sub-auroral zone station, is positively correlated with the elevation of the visual aurora. Furthermore, the luminosity of the visual aurora is positively correlated with the *fEs* (KNECHT [11], OMHOLT [12]).

The ionization in the auroral ionosphere has also been studied by "back-scatter"-techniques, using very high frequencies (LEADABRAND et al [13]). It was shown that the majority of the scatter-echoes originates from an altitude of approximately 100 km, near the maximum of auroral luminosity. This indicates that the height of maximum electron density in the *Es* region is close to the height of maximum luminosity of the visual aurora.

The close relationship between the night-time *Es* layer, the visual aurora and the geomagnetic storm suggests that the three phenomena are due to the same sources of ionization, probably charged particles of solar origin. It has recently been shown (MCILWAIN [14]) that the incidence of visual aurora is associated with influx of electrons at the energy level of 10—20 keV.

In the following sections the relationships between the *visual auroral zone*, the

geomagnetic auroral zone (zone of maximum storminess) and the *sporadic E auroral zone* (zone of maximum *Es* ionization during the night) will be discussed.

3. **The different Es types observed in and near the visual auroral zone.** Before the International Geophysical Year (*IGY*) the routine scaling of the ionosonde records was limited to the virtual heights and the maximum plasma frequencies of the layers *E*, *Es*, *F1* and *F2* and the transmission factor. These parameters give valuable information on the regular layers and are sufficient for practical purposes. Due to the complexibility of the sporadic *E* trace, however, two parameters are far from sufficient for a proper description of this trace.

In order to increase the amount of information on the *Es* traces in the routine, monthly ionospheric bulletins, a new scaling procedure was recommended by the World Wide Sounding Committee (WWSC) of URSI during the IGY. In addition to the virtual height and the maximum plasma frequency, two new parameters were introduced [15], the "*blanketing frequency*" and the "*type of Es*".

The distinction between the different types of *Es* is based upon the appearance of the sporadic *E* traces on the ionosonde records. The *Es* traces have been separated into eight different groups [16]. Typical examples of the *Es* types observed in the auroral zone of *Es* and in the middle latitude zone are shown in Fig. 2. The scaling is frequently made difficult due to: (i) spread echoes, (ii) simultaneous occurrence of different types, (iii) high degree of absorption, and (iv) records of low quality. Furthermore, the variety of *Es* traces observed in and near the auroral zone often makes it difficult to find an adequate type description.

3.1 *Diurnal variation in the occurrence of different Es types.* The ionosonde records obtained at Kjeller and Tromsø during 1957 and 1958 have been rescaled, as far as *Es* types are concerned, in order to ensure identical scaling. The percentage occurrence of the different *Es* types at the two stations is given in Table 2. In order to avoid confusion, the type *l* has been included in the *f*-group in this table. No distinction has been made between *Es* type *r* and "*night-E*" in this table, nor in the following sections.

Table 2. Percentage occurrence of the different *Es* types as observed at Kjeller and Tromsø during 1957 and 1958.

	r	*a*	*f* + *l*	*c*	*h*
Kjeller	0.3	< 0.1	29.3	16.8	< 0.1
Tromsø	38.1	< 0.1	33.8	0.7	< 0.1

Table 2 clearly demonstrates that the *Es* ionization in the auroral zone mainly gives rise to *r*- and *f*-traces on the ionosonde records, whereas the ionization at middle latitudes most frequently is of the *c*- and *f*-type. It has been shown by BECKER [5] that

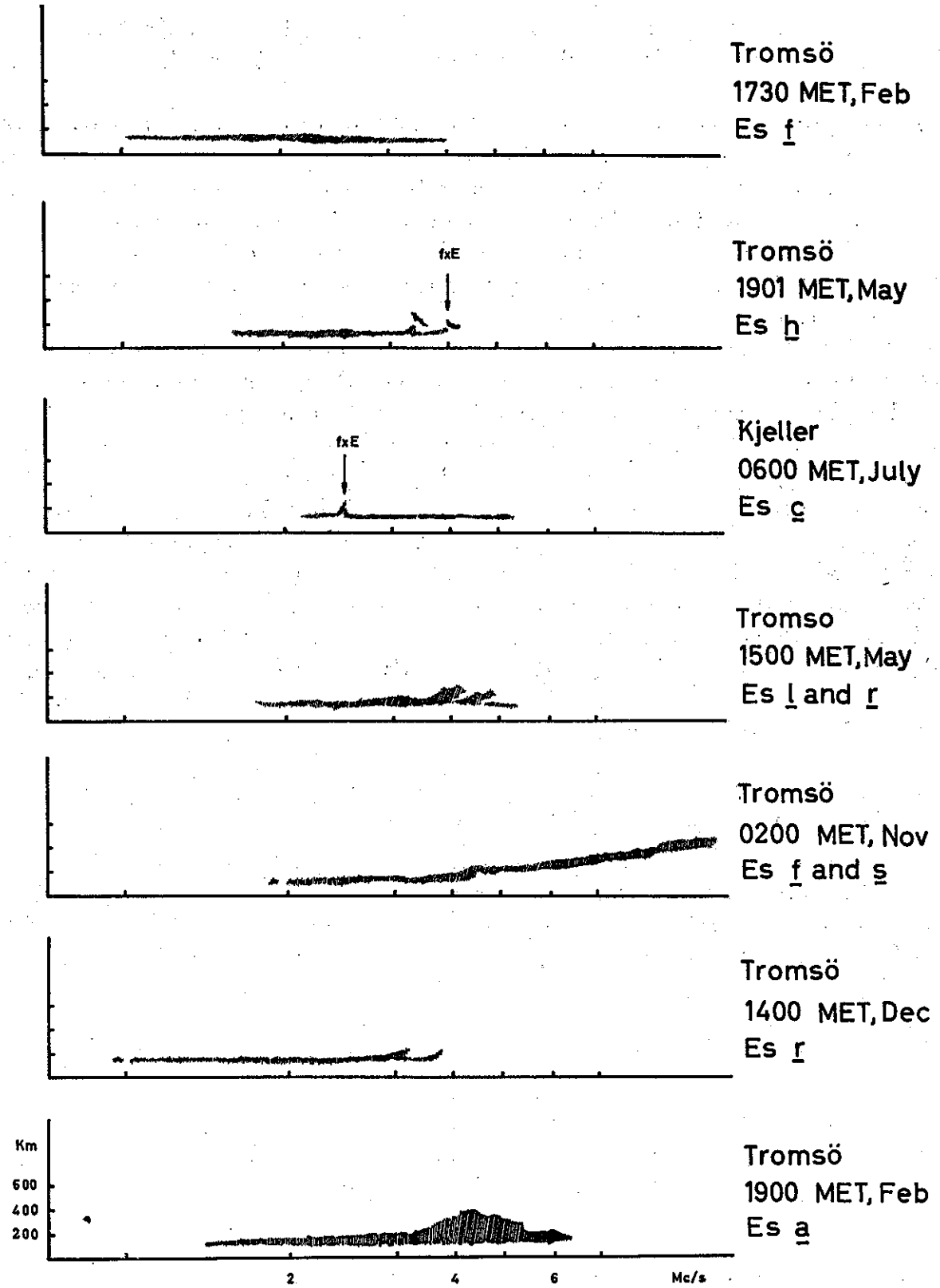

Fig. 2. The seven different *Es* types observed at middle latitudes and in the auroral zone (Redrawn from original records).

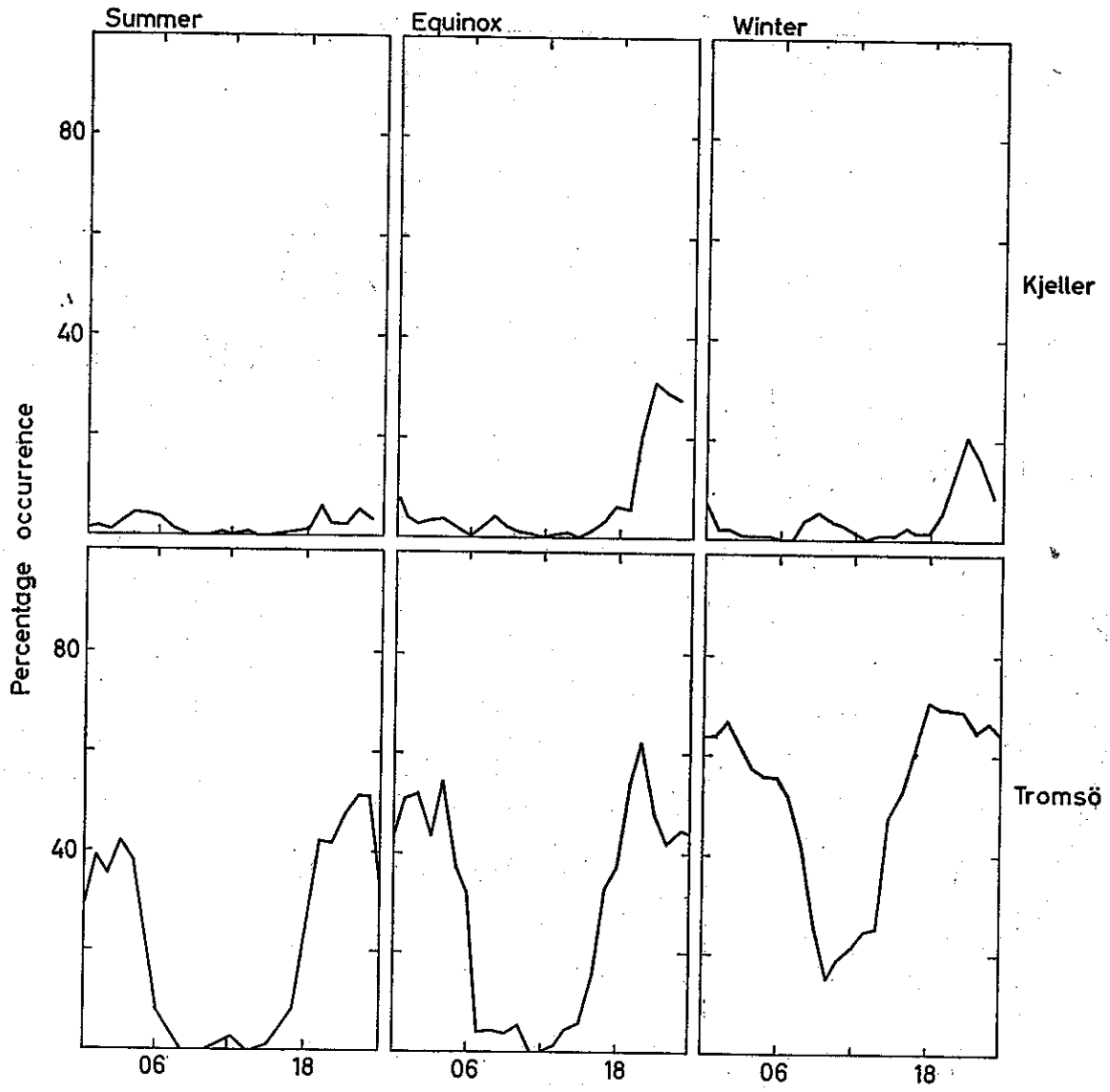

Figure 3.a. Percentage occurrence of the *Es* type *r* as observed at Kjeller and Tromsø during 1957 and 1958.

the types *c* and $f + l$ are completely prevailing at the middle latitude station Lindau, Germany, which is in accordance with our result for Kjeller. The *Es* type *h* has scarcely been observed in Norway.

Type *a* ("*auroral*"), which is supposed to be an auroral zone phenomenon exclusively, is rarely observed at the stations. This is somewhat unexpected, as Tromsø is situated only 1—2 degrees south of the zone of maximum activity of visual aurora. When types *r* and *f* occur simultaneously, which is often the case at Tromsø, they may look like type *a*. In order to obtain a "logical" type description, however, this configuration of *Es* traces was only scaled as type *a* during hours when the types *r* and *f* were not distinguishable due to very spread echoes.

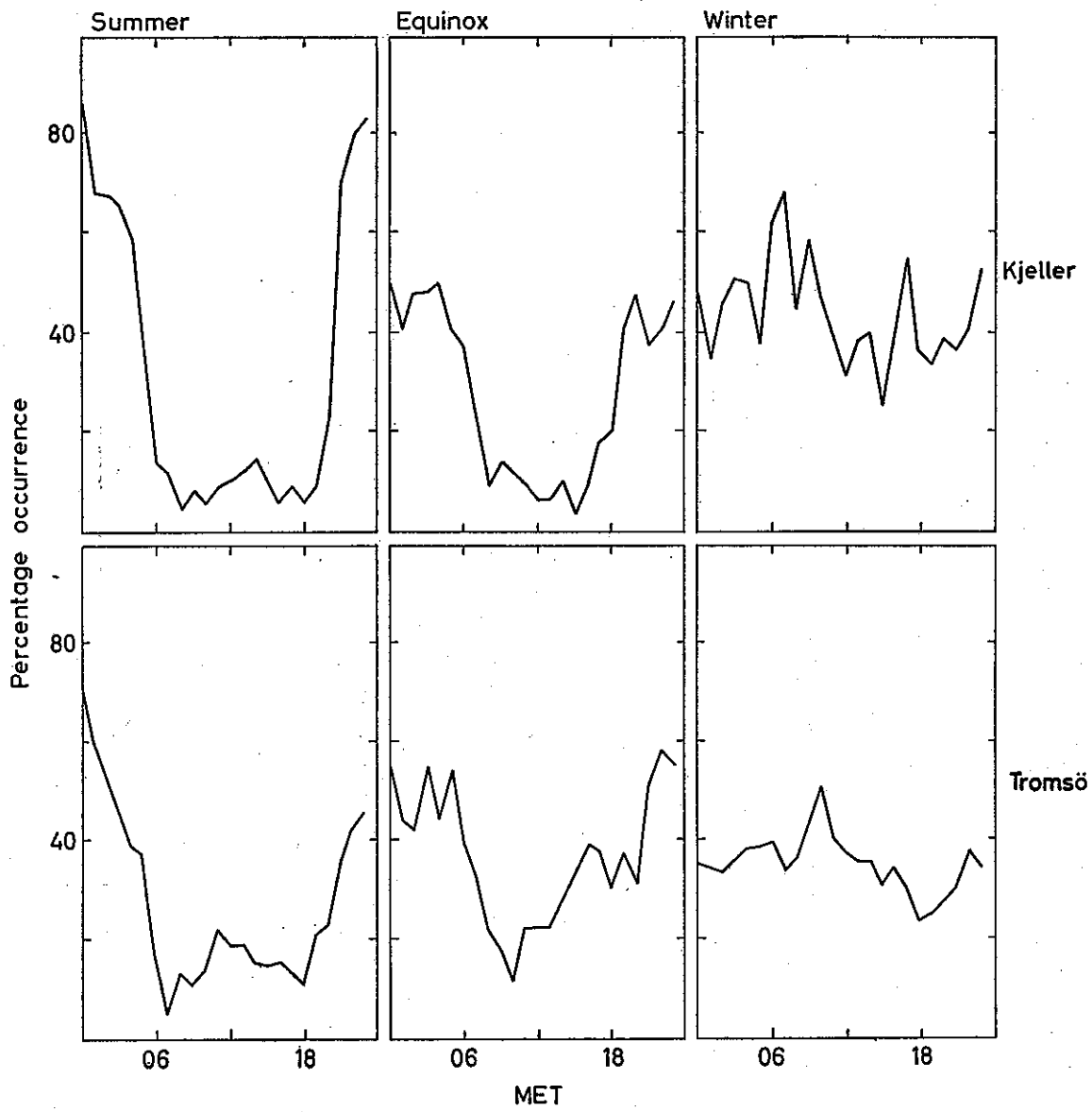

Figure 3.b. Percentage occurrence of the *Es* type *f* as observed at Kjeller and Tromsø during 1957 and 1958.

The study reported in this paper is mainly confined to type *f* (including type *l*) and type *r*. The observed diurnal variation of the occurrence of the two types during 1957 and 58 is shown in Fig. 3 for each season and each station separately.

Type *r* is mainly observed during the night at both stations, with a maximum of occurrence 3—4 hours before local midnight at Tromsø, somewhat later at Kjeller. A secondary maximum is found 3—4 hours after midnight at Tromsø. Type *r* is more frequently observed during the winter than during the summer.

The Es type *f* (*f* and *l* according to the terminology of the WWSC) is a night-time phenomenon at both stations during the summer and the equinoctial months, with a

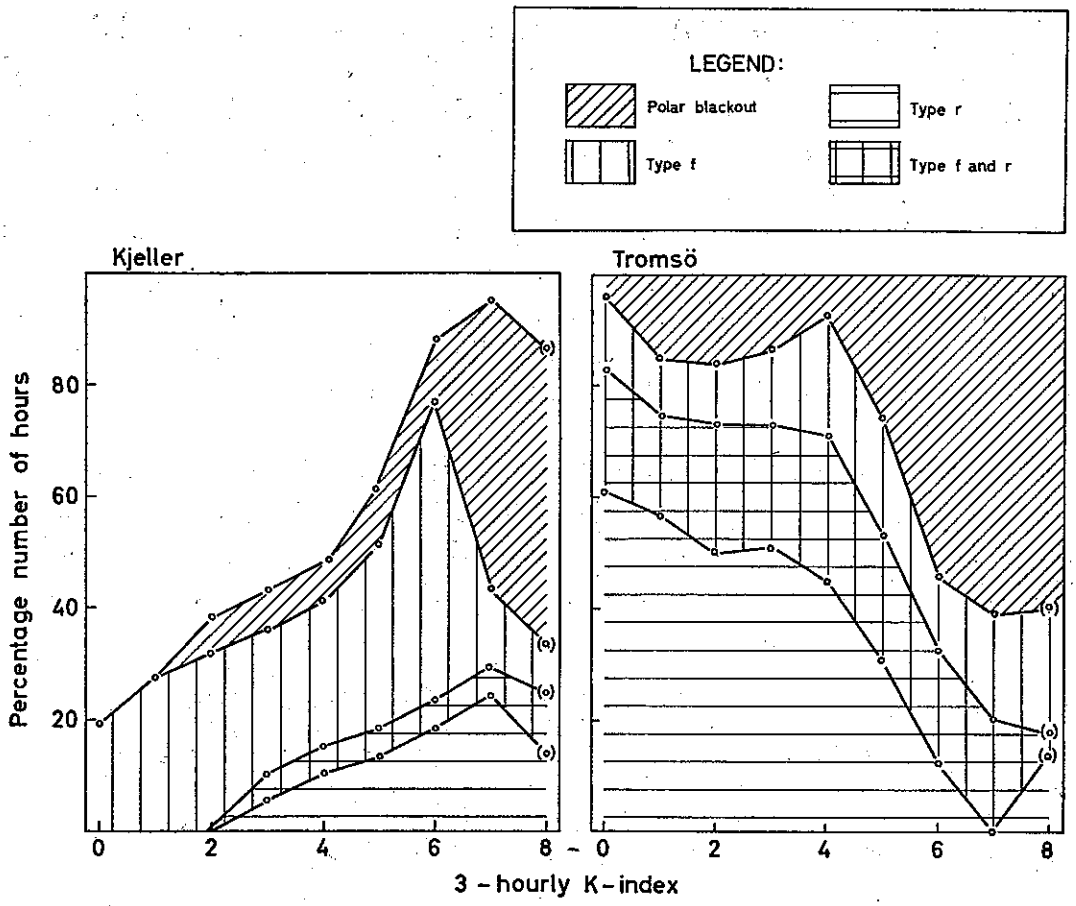

Figure 4. Percentage occurrence of the different *Es* types during equinoctial night-time at Kjeller and Tromsø as a function of magnetic activity.

maximum of occurrence near local midnight. During the winter, however, no clear diurnal variation is found.

Type *r* is much more frequently observed at Tromsø than at Kjeller, whereas the percentage occurrence of type *f* is almost the same at both stations.

3.2 *The relation between the occurrence of different types of Es and magnetic activity.* The occurrence of the different *Es* types during different geomagnetical conditions has been studied, and some results are given in Fig. 4. This figure is based upon the *Es* observations obtained from 2100 to 0300 MET during the equinoctial months of 1957 and 1958 at Kjeller and Tromsø.

A clear, positive correlation is found between the geomagnetic activity and the occurrence of the sporadic *E* type *r* at Kjeller. The percentage occurrence of type *r* increases from 0 during quiet conditions ($K \leqq 2$) to approximately 20 during disturbed conditions ($K \geqq 7$). From a detailed study of the variation of the geomagnetic storm vector observed at Tromsø, it was shown that type *r* was observed at Kjeller only during hours when the geomagnetic storm current system was situated some distance south of Tromsø.

At Tromsø (Fig. 4) the sporadic *E* type *r* is most frequently observed during hours with low magnetic activity. The percentage occurrence decreases from 70—80 during quiet conditions ($K \leqq 2$) to approximately 20 during disturbed hours ($K \geqq 7$). The frequency of occurrence of polar blackout increases with magnetic activity, as indicated in the illustration. The negative correlation between the *K*-index and the occurrence of *Es* type *r* can, however, not be ascribed to absorption effects only, as will be shown in Section 6.

The incidence of the sporadic *E* type *f* seems to be unaffected by variations in the geomagnetic field both at Tromsø and at Kjeller. The percentage occurrence of this type is approximately 30 during disturbed as well as quiet nights at both stations.

4. Large-scale structure of the sporadic E auroral zone. In order to study the "large scale" structure of the sporadic *E* auroral zone in more detail, two ionosonde field stations were set up in northern Norway during September 1959. The stations were located 100 km east of Tromsø and 100 km south of Tromsø, respectively (Vide

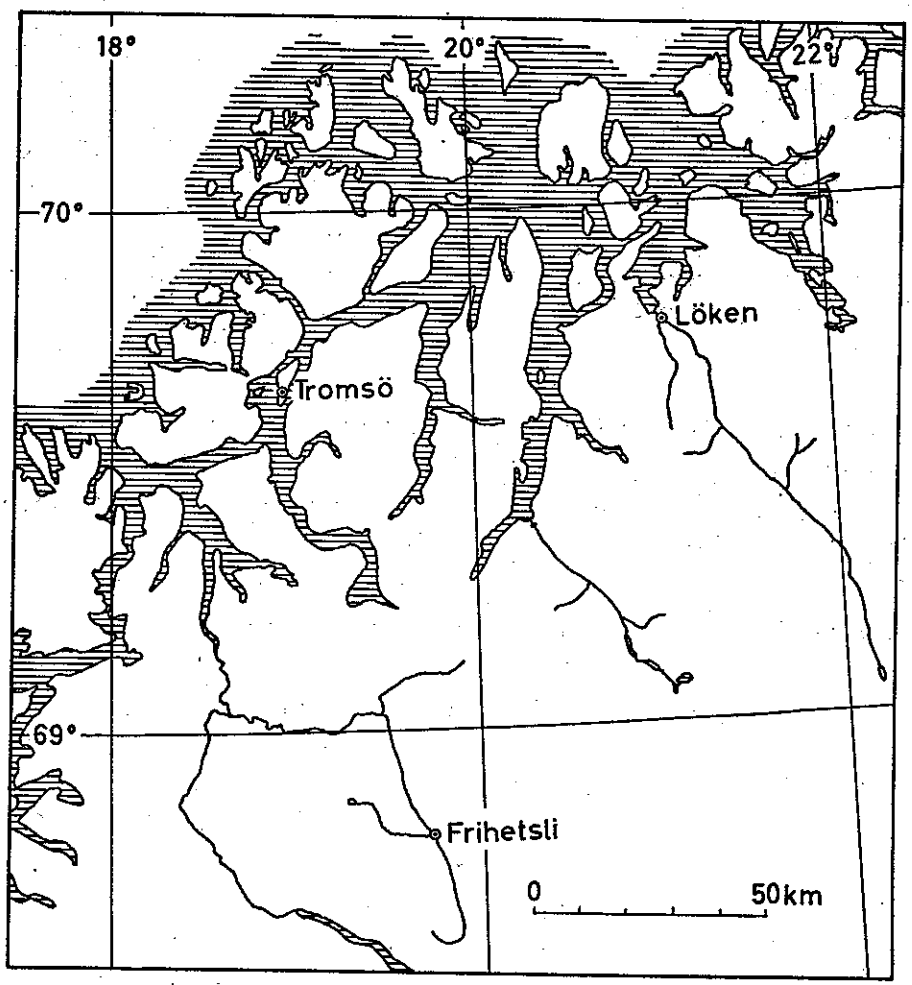

Fig. 5. Location of stations.

Fig. 5). At the two field stations and at the ionosonde station in Tromsø, the same type of equipment [19] and an identical antenna arrangement (parallel delta-antennas for transmission and reception) was used. The stations were in operation every night from 28 September through 2 November 1959, taking records every 15 minutes. During seven selected nights the time separation between consecutive recordings was only three minutes.

The records from this experiment were carefully analysed in order to study the different *Es* types separately. In the following sections the top frequency of the *Es* type *r* is indicated by f_rEs, and the top frequency of the nonretardation traces is referred to as f_nEs. (The latter group thus includes the types *l*, *f*, *h* and *a*.)

A typical record obtained during this period is given in Fig. 6, showing two types of *Es*. The scaled values of f_rEs and f_nEs are also indicated in the illustration.

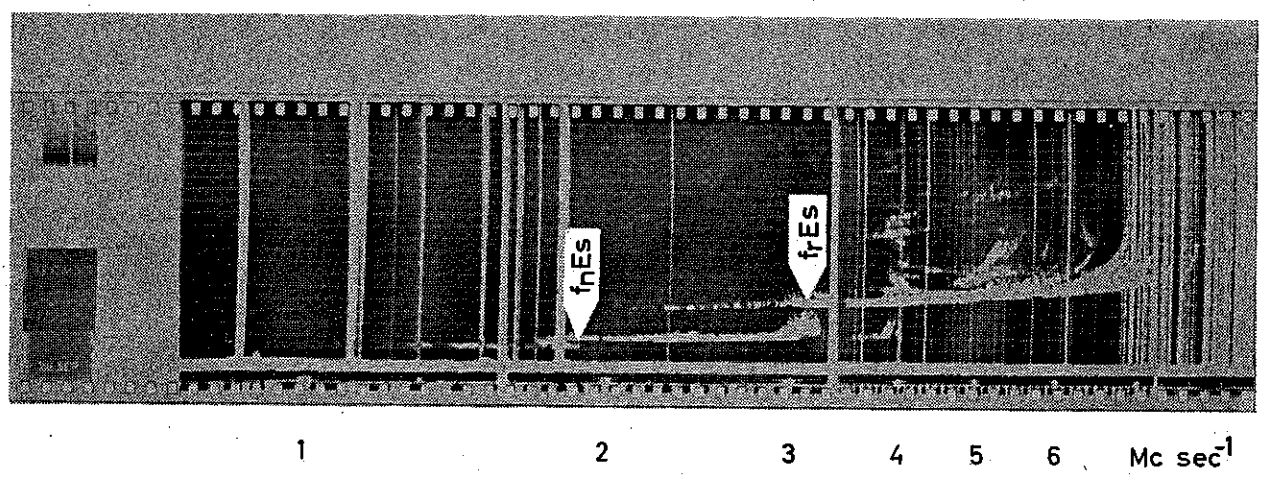

Fig. 6. Typical record.

4.1 *Diurnal variations of f_rEs and f_nEs.* The experiment demonstrated that the time and spatial variations of f_rEs differ significantly from the time and spatial variations of f_nEs. The f_rEs varies in a smooth way with few rapid or large changes during the night. The f_nEs, however, seems to vary quite erratically. In fact, this parameter may change more than 7 Mc sec^{-1} within a quarter of an hour, and the correlation coefficient between consecutive observations of f_nEs at time intervals of three minutes is less than *0.4*.

The variation of f_nEs and f_rEs during two selected nights is shown in Fig. 7. Fig. 7a corresponds to a geomagnetically quiet night, whereas Fig. 7b refers to a strongly disturbed night. In accordance with Fig. 4 the retardation type is present only during quiet conditions. The non-retardation trace is, however, observed both nights.

The period of observation was very quiet geomagnetically, and the retardation type of *Es* was observed more than 85 per cent of all night hours. The mean percentage occurrence of the non-retardation type of *Es* was approximately 25 for all the nights of observation, the maximum of occurrence being near 2130 MET.

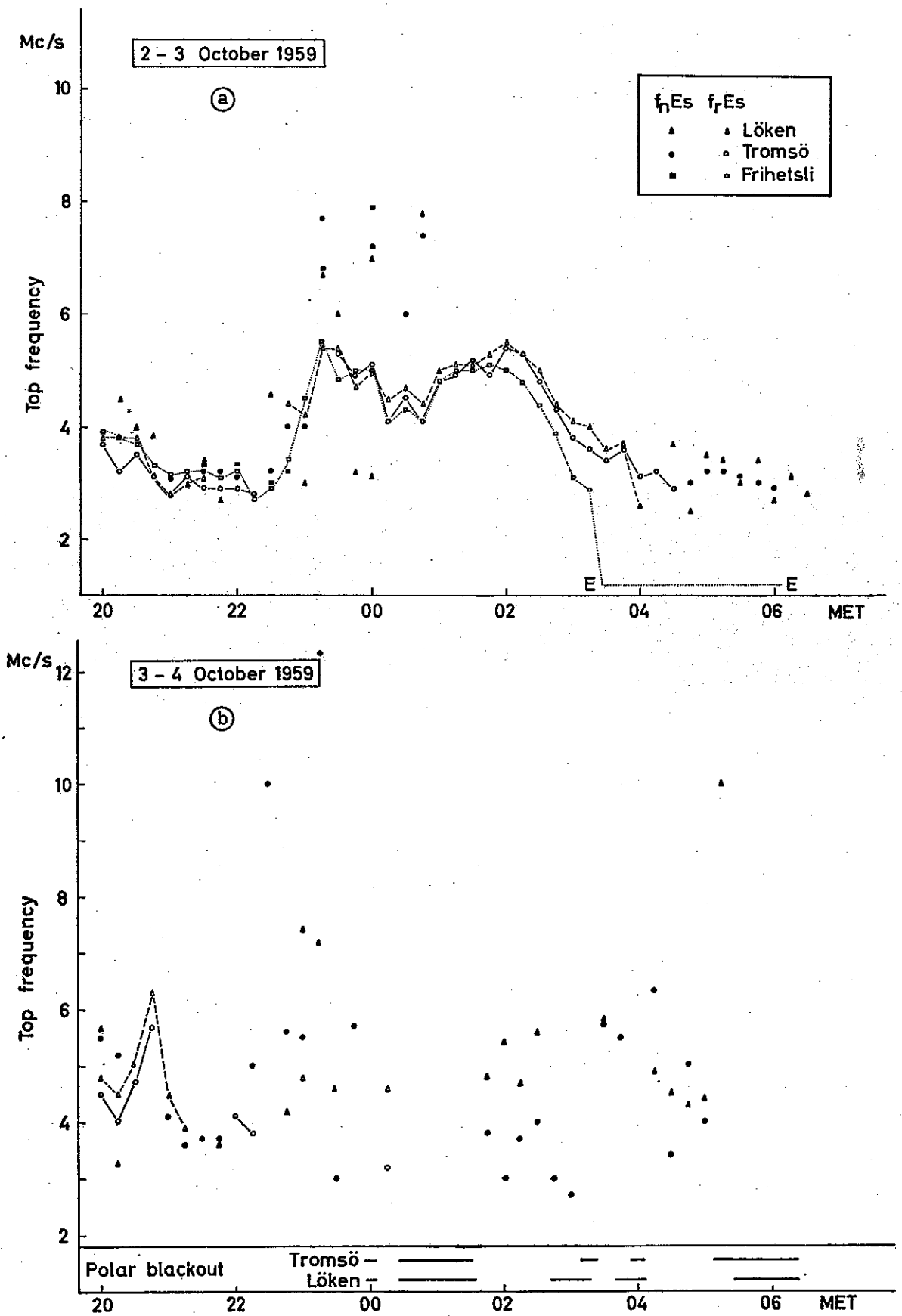

Fig. 7. Diurnal variation of f_nEs and f_rEs during two selected nights for the three stations.

4.2 *Spatial variations of $f_r Es$ and $f_n Es$.* The diurnal variation of $f_r Es$ at the three stations showed remarkably similar trends, the simultaneously observed values at Tromsø and Løken being practically identical. The distribution function of the difference between corresponding values at the three stations is given in Fig. 8. The difference between the $f_r Es$ at Tromsø and at Løken was less than 0.3 Mc sec^{-1} during 75 % of all hours of observation. Thus, the ionization in the auroral ionosphere which gives rise to the *r* type of *Es* on the ionograms is very uniform over large areas.

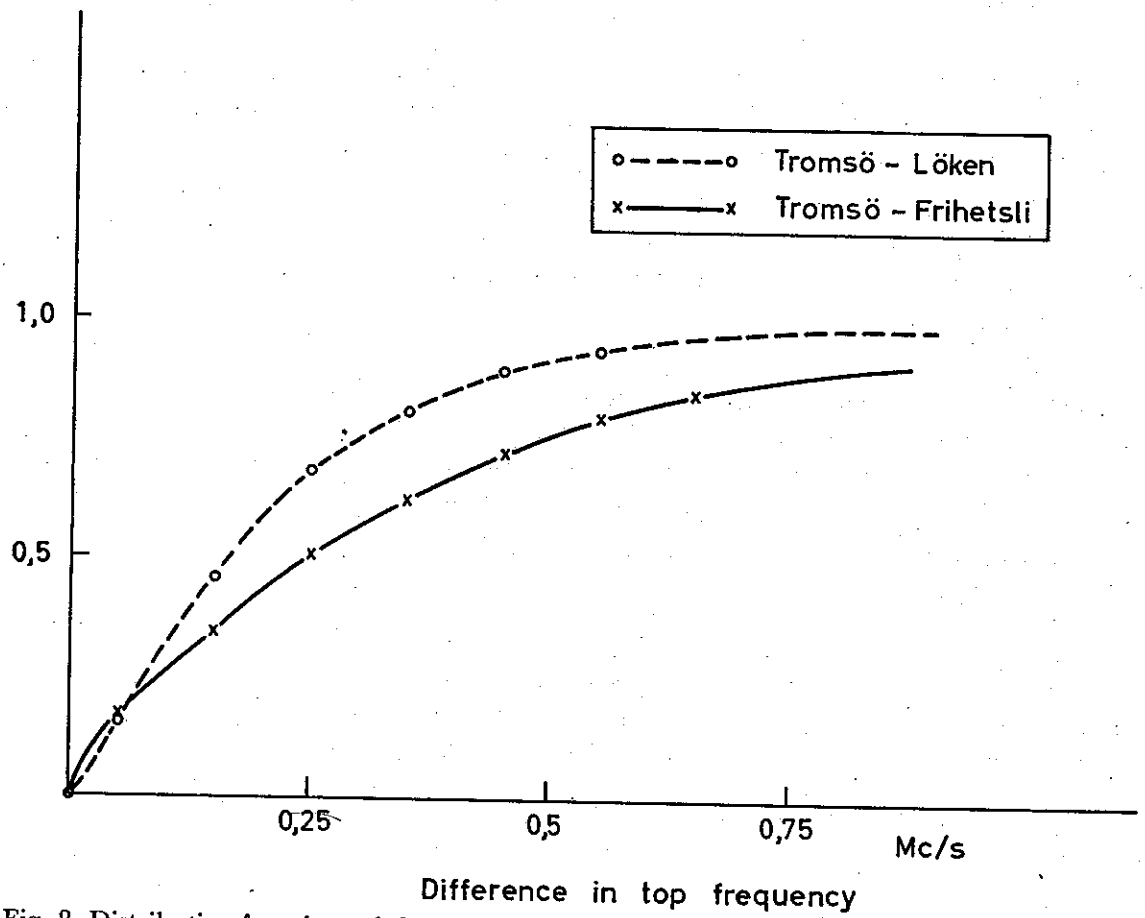

Fig. 8. Distribution functions of the differences between simultaneously observed values of $f_r Es$.

Fig. 8 seems to indicate that the ionization in the sporadic *E* auroral zone associated with *Es* type *r* is more uniform in the east-west direction than in the north-south direction. This is furthermore supported by the fact that the correlation coefficient between Tromsø and Frihetsli, which is in the range 0.85—0.90, is somewhat lower than the correlation between Tromsø and Løken, which is higher than 0.95. However, a more detailed study made it clear that the difference between the east-west direction and the north-south direction is an effect caused by the latitudinal limitation of the sporadic *E* auroral zone rather than a non-isometrical structure of the ionization in this zone. During hours when the *Es* auroral zone was situated above all

stations, the f_rEs was practically identical at the stations. During the morning hours, however, when the visual auroral zone moved northward, the observed value of f_rEs was essentially lower at Frihetsli than at the other stations (Vide Fig. 7a).

The spatial correlation of the f_nEs is much lower than the correlation of the f_rEs. In fact, the percentage occurrence of simultaneous observations of the non-retardation type of *Es* at two or three stations is only slightly higher than could be expected by pure chance (Table 3). It may therefore be concluded that the mean horizontal extent of the irregularities in the *Es* region associated with the non-retardation trace is less than 100 km.

The diurnal variation of f_nEs at the three stations has been compared carefully in order to trace possible drift effects of the large scale irregularities in the sporadic *E* region. This method is not well suited for studying velocities in the range 1000—2000 m sec^{-1}, which are observed in the auroral ionosphere (BULLOUGH and KAISER [20]), due to the large time separation between the recordings. It seems improbable, however, that the rapid variation of the f_nEs may be ascribed to bodily drifting irregularities in the *Es* region, only.

Table 3. The percentage occurrence of the non-retardation type of as *Es* observed at the three stations Tromsø (T), Løken (L) and Frihetsli (F).

Observed	Pure chance probability (per cent)
P (T) = 25 P (L) = 33 P (F) = 19	
P (T and L) = 13 P (T and F) = 8 P (L and F) = 7	P (T and L) = P (T) · P (L) = 8 P (T and F) = P (T) · P (F) = 5 P (L and F) = P (L) · P (F) = 6
P (T and L and F) = 5	P (T) · P (L) · P (F) = 2

The observed distributions of f_rEs and f_nEs for Tromsø are given in Fig. 9. The median of f_nEs, approximately 5.7 Mc sec^{-1}, is distinctly higher than the median of f_rEs, which is approximately 4.1 Mc sec^{-1}. Furthermore, the observed values of f_nEs show a much higher degree of scatter than those of f_rEs.

An interesting feature of the distribution function of the f_rEs is the abrupt cut-off near 6 Mc sec^{-1}. In fact, values of f_rEs greater than 6.3 Mc sec^{-1} were not observed during the whole period of observation. This point ought to be compared with results from auroral scatter experiments, which indicate that "the average ionization density in most auroras does not exceed about $5 \cdot 10^5$ electrons per cm^3" (NICOLS [21]). This value corresponds to a plasma frequency of 6.3 Mc sec^{-1}. The apparent "upper limit" of f_rEs will be discussed in Section 6.

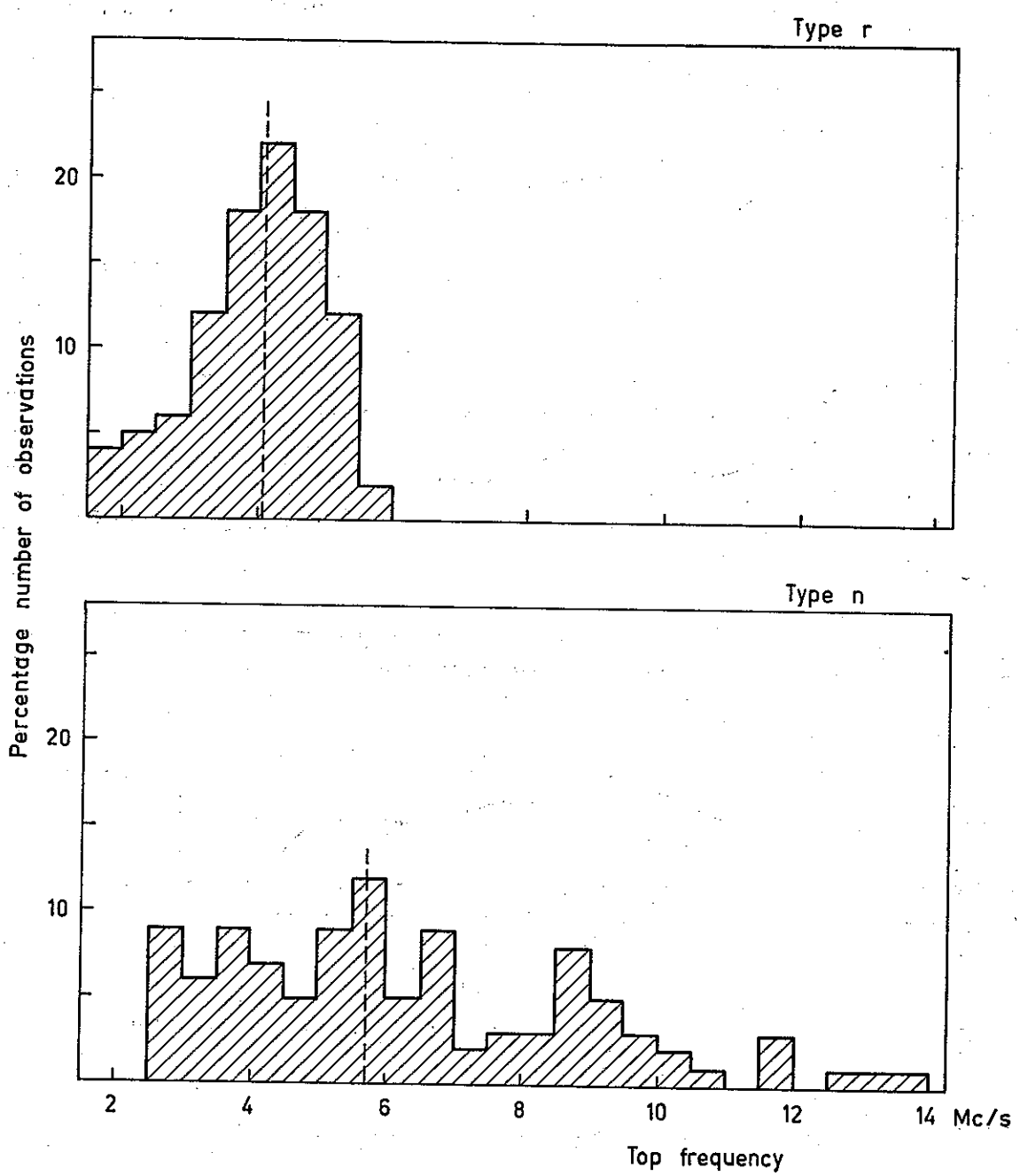

Fig. 9. Observed distribution of f_rEs and f_nEs (Tromsø-values).

5. Variations in the maximum plasma frequency of the sporadic E layer in the auroral zone. The mean northerly and southerly boundary of the sporadic E auroral zone is 73° and 63° geom lat, respectively (MATSUSHITA [22]). The diurnal variation of this zone is, however, not well known.

In this section results will be given from a study of the time variations in the sporadic E auroral zone above Scandinavia. The relation between the variation of the sporadic E auroral zone and the geomagnetic auroral zone will also be discussed.

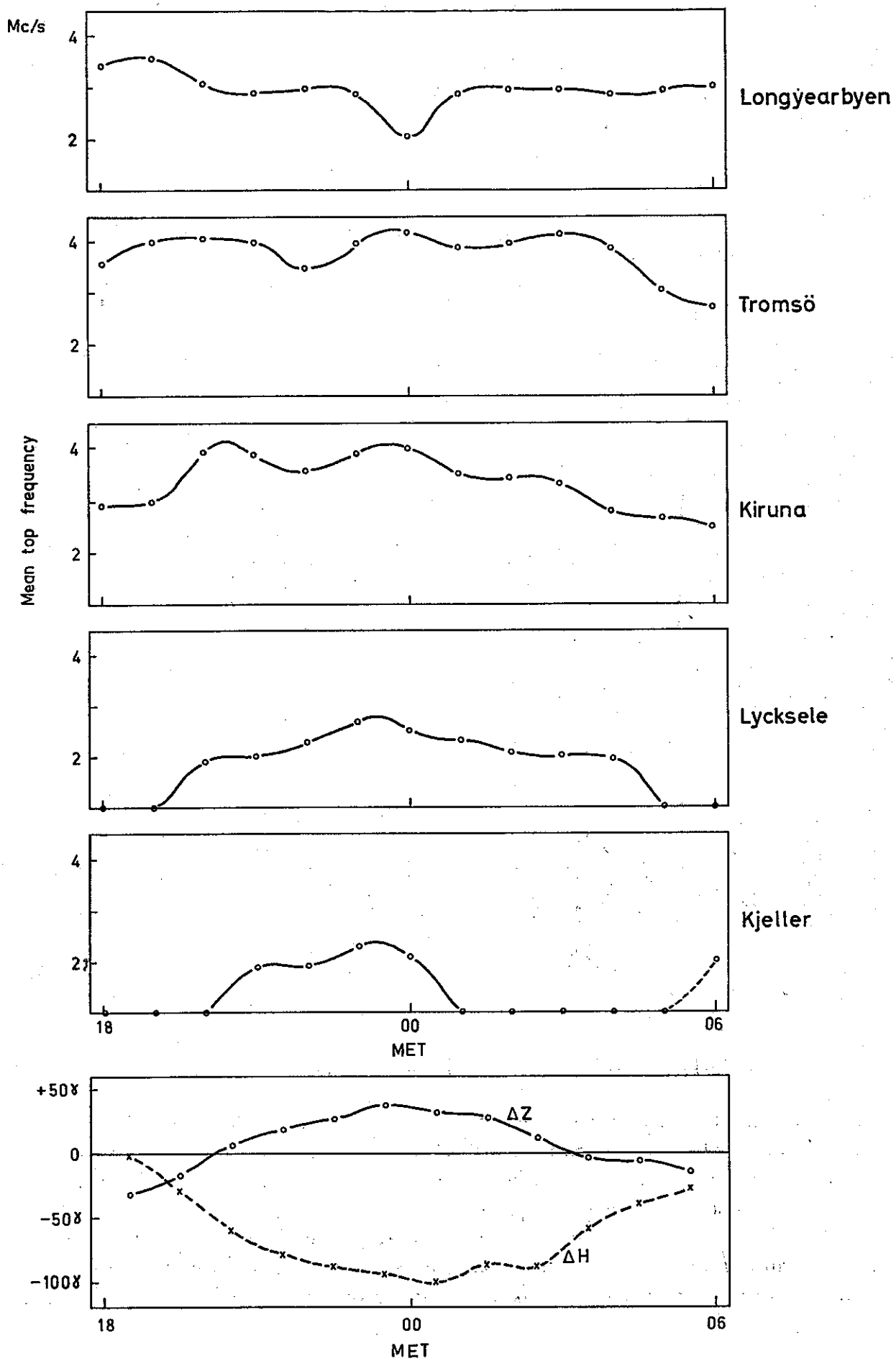

Fig. 10. Mean time variation of *fEs* at some Scandinavian stations during the period November 1957—February 1958.

5.1 *Diurnal variations of fEs near the auroral zone.* As previously mentioned, the variation of *fEs* in the auroral zone normally seems to be quite erratic. From the mean nightly variation of this parameter for several nights, however, certain regular features may be traced.

The mean nightly variation of *fEs* as observed at some Scandinavian stations from November 1957 through February 1958, is given in Fig. 10. The mean variation of the horizontal ($\triangle H$) and vertical ($\triangle Z$) component of the geomagnetic storm vector (HARANG et al [23]) at Tromsø during the same period is also shown in this illustration.

The mean, nightly value of *fEs* decreases with increasing distance from the auroral zone (Fig. 10). At Tromsø the mean of *fEs* exceeds 3 Mc sec^{-1} during all night hours, whereas the mean at Kjeller is less than 2 Mc sec^{-1} at practically all hours.

An interesting point is the "phase" difference between the stations south of the auroral zone and those north of the auroral zone near local midnight. Near midnight a clear maximum is observed at the four stations situated south of the visual auroral zone, whereas a minimum is found at Longyearbyen. This is a consequence of the meridional shift of the position of the sporadic *E* auroral zone during the night. In the following sections it will be shown that the sporadic *E* auroral zone is closely related to the geomagnetic storm current systems. The mean variation of the geomagnetic storm vector at Tromsø during the same period (Fig. 10, below) indicates that the geomagnetic auroral zone reaches its southernmost position and maximum intensity near midnight. The disagreement between the station north of the visual auroral zone and the stations south of the zone may therefore readily be explained by the southward shift of the sporadic *E* auroral zone near midnight.

Two secondary maxima in the nocturnal variation of *fEs* are observed at Kiruna and Tromsø near 2000—2100 MET and 0300 MET. At these hours the mean storm current is situated above Tromsø ($\triangle Z = 0$), as shown in Fig. 10.

5.2 *Relationship between the geomagnetic auroral zone and the sporadic E auroral zone.* The mean latitudinal variation of *fEs* (midnight values) as observed in Scandinavia during the years 1957—1959 is shown in Fig. 11. This illustration is in fair agreement with the mean latitude variation of *fEs* as deduced from Japanese observations (MATSUSHITA [22]). The *Es* auroral zone is extending in a southerly direction to approximately 63° geom. lat. and the maximum electron density in the zone is found near 66° geom. lat. The percentage occurrence of visual aurora above Scandinavia, as given by VESTINE [24], is also shown in the illustration. The mean visual auroral zone seems to be located 1—2° nearer to the pole than the sporadic *E* auroral zone. As, however, the two curves refer to two different periods of observation, this difference may not be significant. When neglecting this point, there is a fair agreement between the two curves.

In an earlier paper by the author [10] it was shown that the latitude of the maximum of ionization in the sporadic *E* auroral zone decreases with increasing values of the Tromsø *K*-index. In Fig. 12 some results from this study are given. The electron

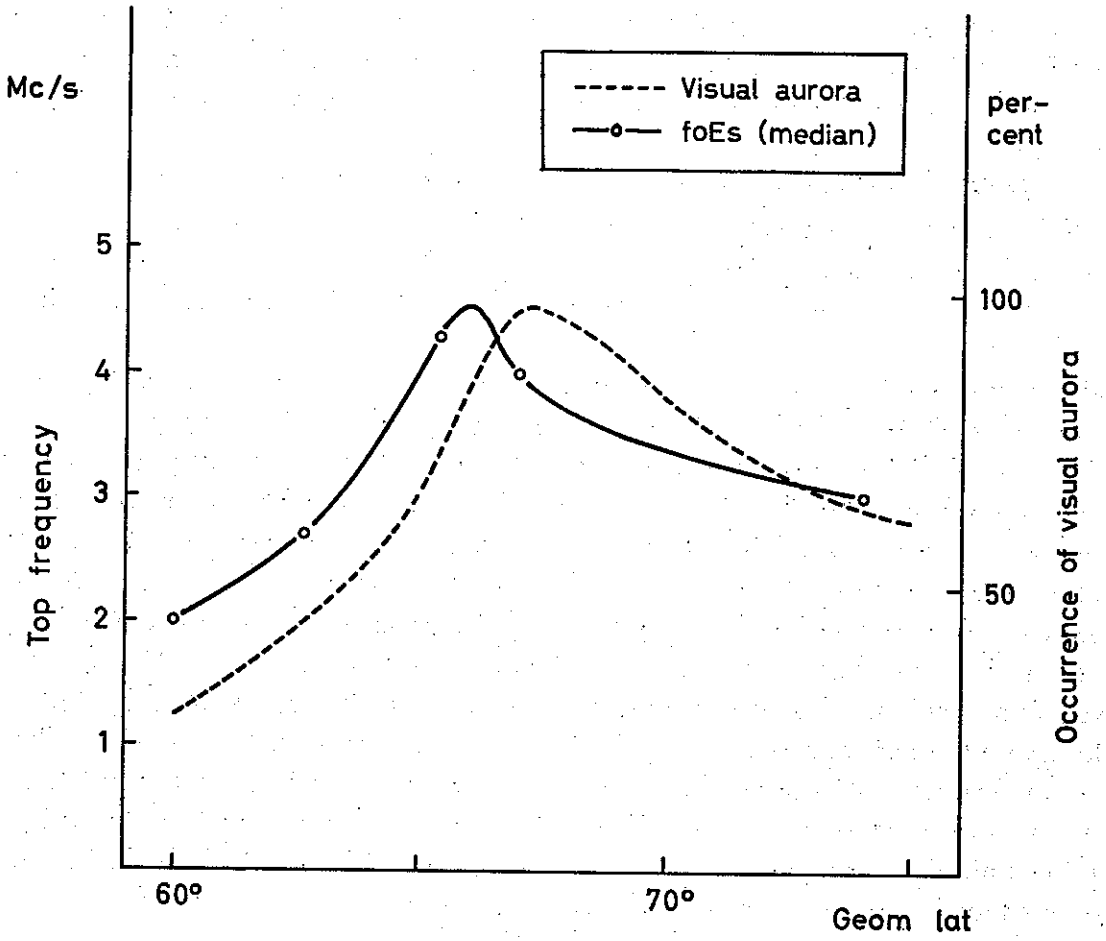

Fig. 11. Mean latitudinal variation of *fEs* (midnight values) during the winter, and percentage number of hours with visual aurora.

density in the middle of the *Es* zone is increased by a factor of 4, when the *K*-index increases from 0 to 6, and the maximum is shifted from approximatety 70° to 65° geom. lat. The results given in Fig. 12 refer to midnight conditions (2200—0200 MET). It is well known that the geomagnetic storm current system in the auroral zone is also shifted towards lower latitudes during disturbed conditions (NAGATA [25]). The mean latitudinal variation of the horizontal component of the storm vector near midnight in Scandinavia during different geomagnetical conditions is shown in Fig. 12b (After HARANG [26]). The latitude of maximum activity is shifted from approximately 69° geom. lat. during quiet conditions (HARANG's Class 2) to 65° geom. lat. during disturbed conditions (HARANG's Class 4), in fair agreement with the meridional shift of the sporadic *E* auroral zone.

The three hourly K-index is a measure of the "scale of variation" for the three geomagnetic parameters (D, Z, H). As the polar magnetic storm is caused by enhanced current density in the auroral ionosphere (CHAPMAN and BARTELS [27]), one might say that the *K*-index is a parameter for the "scale of irregularities" in this ionospheric

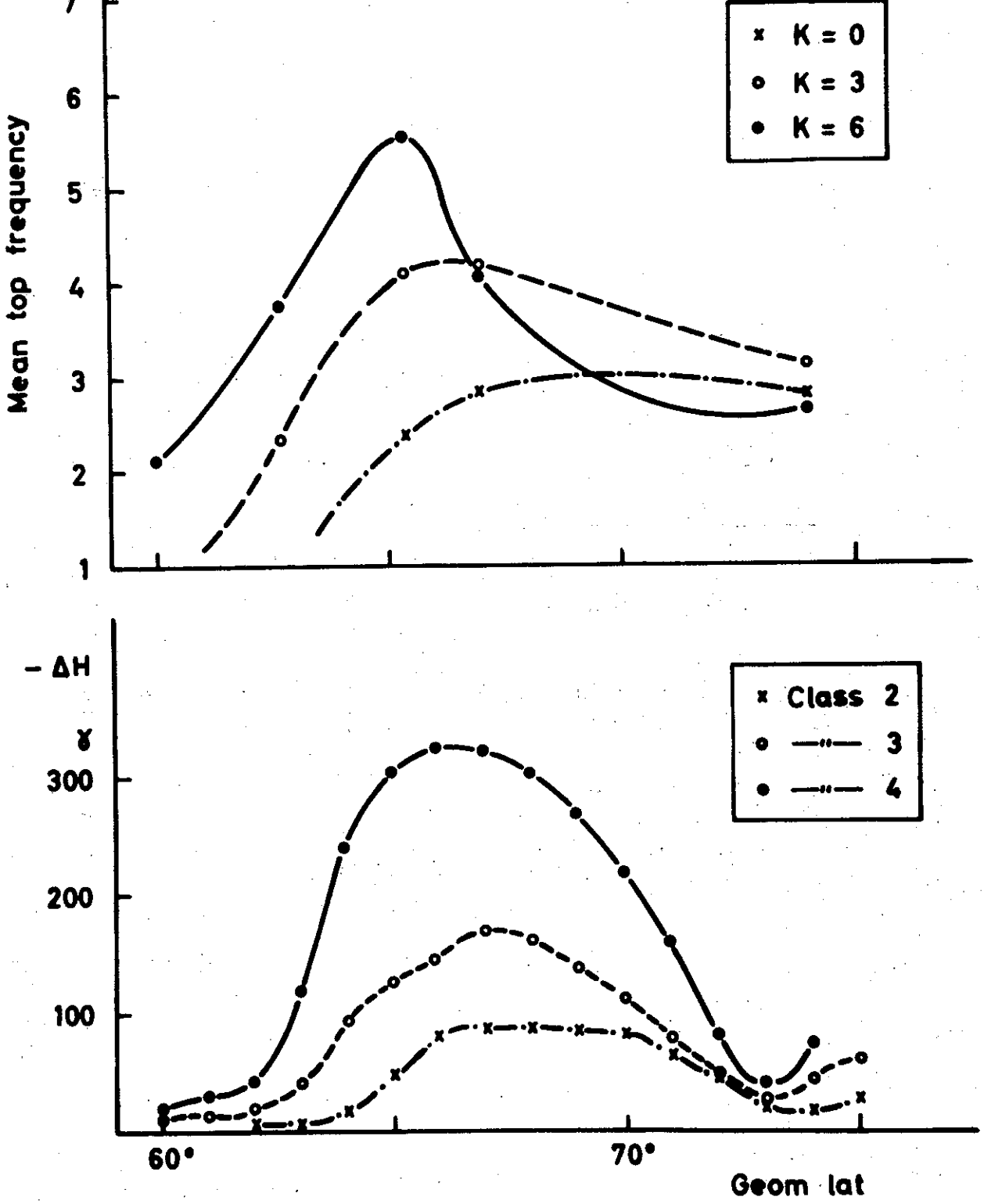

Fig. 12. Mean latitudinal variation of *fEs* and of $\triangle H$ during different storm conditions (See text).

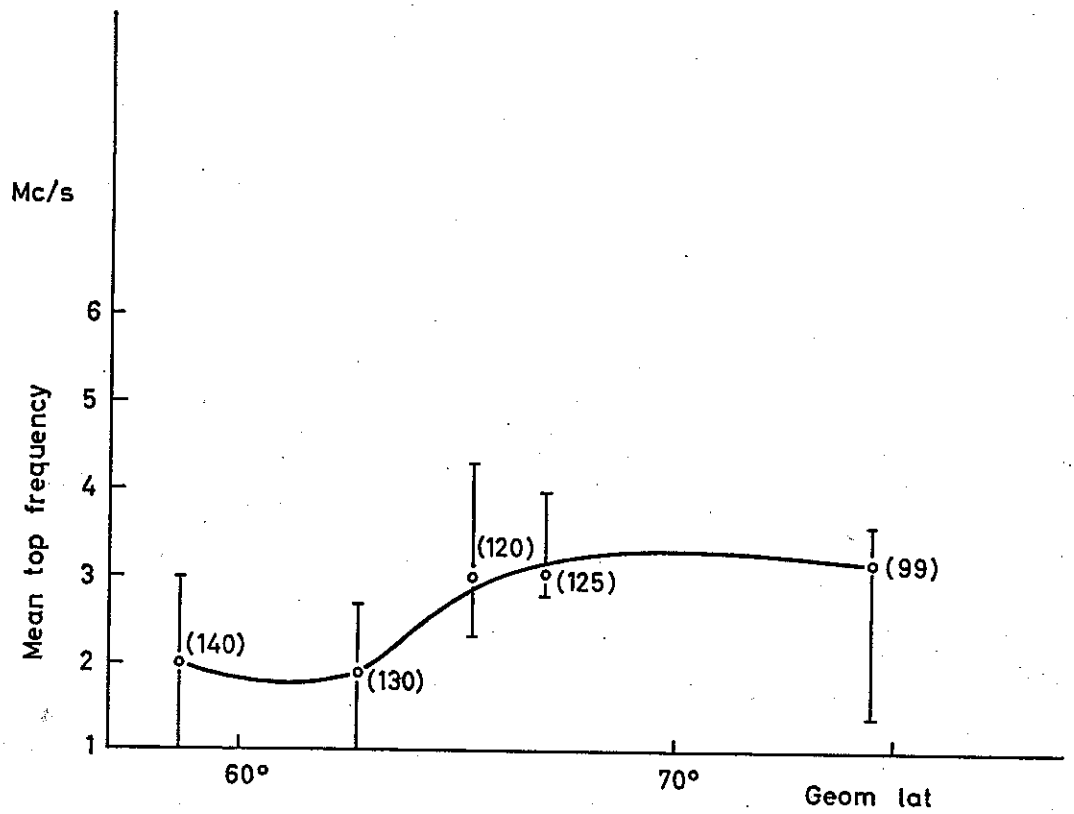

Fig. 13. The latitudinal distribution of *fEs* above Scandinavia during quiet night hours.

current. In order to deduce the position and the intensity of the storm current, it is, however, essential to known the components ($\triangle Z$ and $\triangle H$) of the storm vector as a function of latitude.

Night observations of the geomagnetic storm vector obtained at Tromsø during 1957 and 1958 have been separated into three groups: (1) quiet conditions ($|\triangle F| < 20\ \gamma$), (2) medium disturbed conditions ($-100\ \gamma \leqq \triangle F \leqq -20\ \gamma$) and (3) disturbed conditions ($\triangle F < -100\ \gamma$). The latter two groups have been separated into three subgroups, which refer to different positions of the storm current system (a) current situated far to the south: $\left(\frac{\triangle Z}{\triangle H} < -0.5\right)$, (b) current situated above Tromsø $\left(-0.5 \leqq \frac{\triangle Z}{\triangle H} \leqq +0.5\right)$ and (c) current situated far to the north $\left(+0.5 < \frac{\triangle Z}{\triangle H}\right)$ It is of importance to notice that $\left(\frac{\triangle Z}{\triangle H}\right)$ is frequently positive during the night, even during disturbed conditions.

The mean latitudinal distribution of *fEs* for group (1) is shown in Fig. 13. Even though this group refers to extremely quiet conditions, a considerable amount of free electrons is present in the *Es* region. If the ionization in the sporadic *E* layer in the

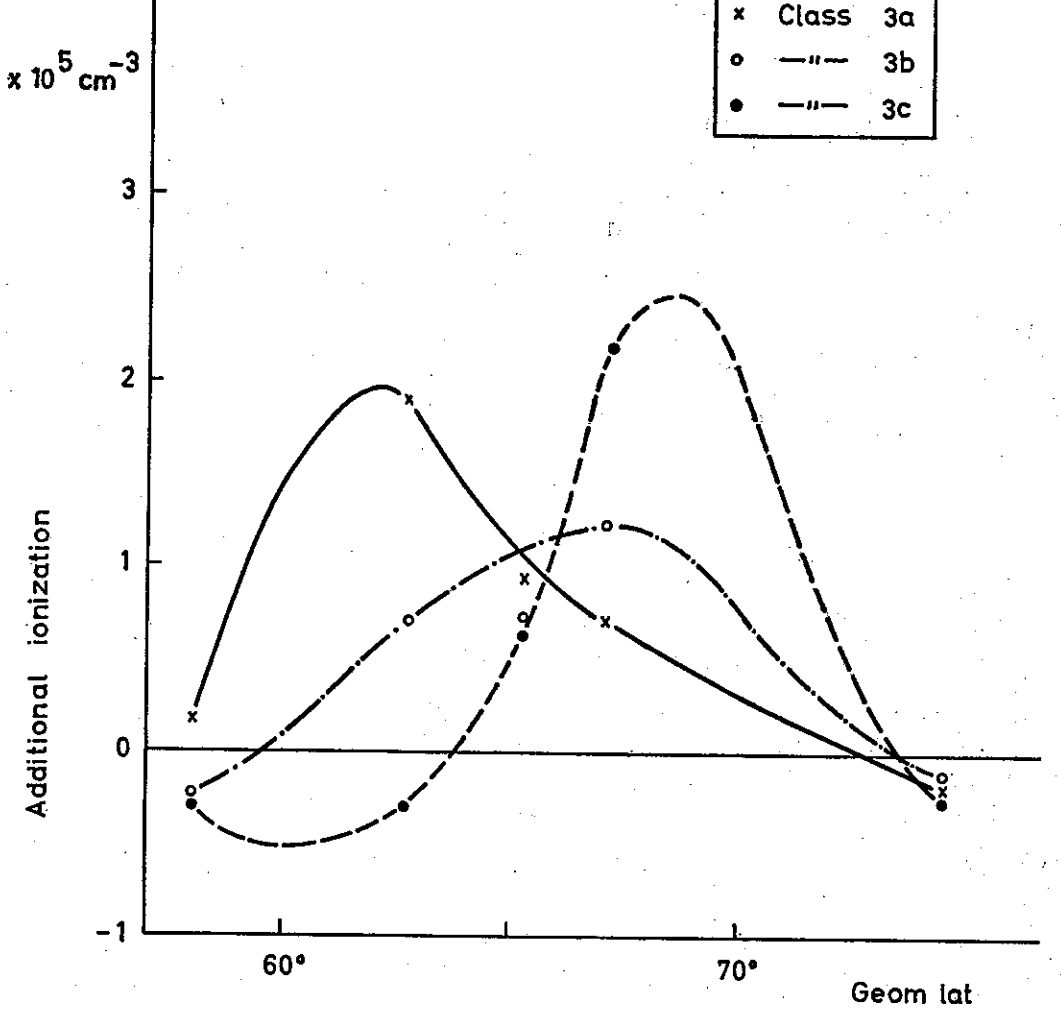

Fig. 14. Additional ionization in the sporadic E region during disturbed conditions (See text):

auroral zone is due to incoming charged particles, this indicates that a certain influx of particles takes place even during quiet periods. The maximum density in the zone, approximately $1.3 \cdot 10^5$ cm^{-3}, is found near 67—70° geom. lat.

During hours with enhanced geomagnetic activity, a clear increase of the electron density in the *Es* region is observed. The amount of increase is, however, strongly influenced by the position of the geomagnetic auroral zone. The mean increment in the maximum electron density of the *Es* layer for disturbed conditions (Groups 3a, 3b and 3c) as function of latitude is shown in Fig. 14.

The most important results of Fig. 14 may be summarized as follows:

a) During hours when the storm current system is situated far to the south, the maximum increase of ionization in the sporadic E region is also observed to the south of Tromsø. For disturbed conditions (Group 3a) the maximum of additional

ionization, amounting to approximately $2 \cdot 10^5$ cm^{-3}, is observed near 62—63° geom. lat. The mean increase during the same hours above Tromsø is only $0.5 \cdot 10^5$ cm^{-3}.

b) During storm hours when the current is situated far to the north (Group 3c), the maximum of additional ionization, approximately $2.5 \cdot 10^5$ cm^{-3}, is found to the north of Tromsø, at 69—70° geom. lat.

c) During hours when the storm current system is above Tromsø ($\Delta Z \approx 0$), the maximum of additional ionization is found near Tromsø. For disturbed conditions (Group 3b) the maximum of additional ionization is of the order $1.2 \cdot 10^5$ cm^{-3}.

Fig. 14 shows that the geomagnetic changes observed at ground are largely controlled by the position and intensity of the sporadic *E* auroral zone. This lends strong support to the assumption that the electrons in the *Es* layer are part of the geomagnetic storm current.

6. Discussion of results.

6.1 *Morphology of the two types of Es observed in the auroral zone.* The statistical study reported in the present paper shows that a fairly thick, uniform layer is present at the 100 km level during most winter nights in the auroral zone. The latitudinal extent of this layer is relatively well defined. The northern boundary of the layer varies from 65 to 73° geom. lat. during different geomagnetical conditions, and the southern boundary from 58 to 67° geom. lat.

During geomagnetically quiet periods this "*sporadic E auroral zone*" is situated to the north of Tromsø. During magnetic storms (high *K* values), the zone is frequently shifted towards much lower latitudes. This explains why the correlation between the *K*-index and the occurrence of *Es* type *r* is positive at Kjeller and negative at Tromsø. For stations situated in the transition region between the auroral zone and the middle latitude zone, one would expect a maximum occurrence of *Es* type *r* during medium disturbed conditions. Unfortunately, proper data from a transition station have not been available during this study. However, recently published results from the sub-auroral zone station Halley Bay (Antarctica) demonstrate that this assumption is correct. The percentage occurrence of *Es* type *r* at this station is shown in Fig. 15 (After Bellchambers and Piggott [18]).

From a detailed study it was shown that the position of the sporadic *E* auroral zone is closely related to the position of the geomagnetic storm current system. Some of the regular variations of the *fEs* near the auroral zone may be associated with regular meridional movements of the geomagnetic auroral zone. During the early evening hours, the electron density in the mean sporadic *E* auroral zone is relatively low, the maximum being situated north of Tromsø. Towards midnight the electron density in the zone increases, and the maximum is shifted towards lower latitudes. Around 2000—2100 MET, when the mean storm current system is situated above Tromsø,

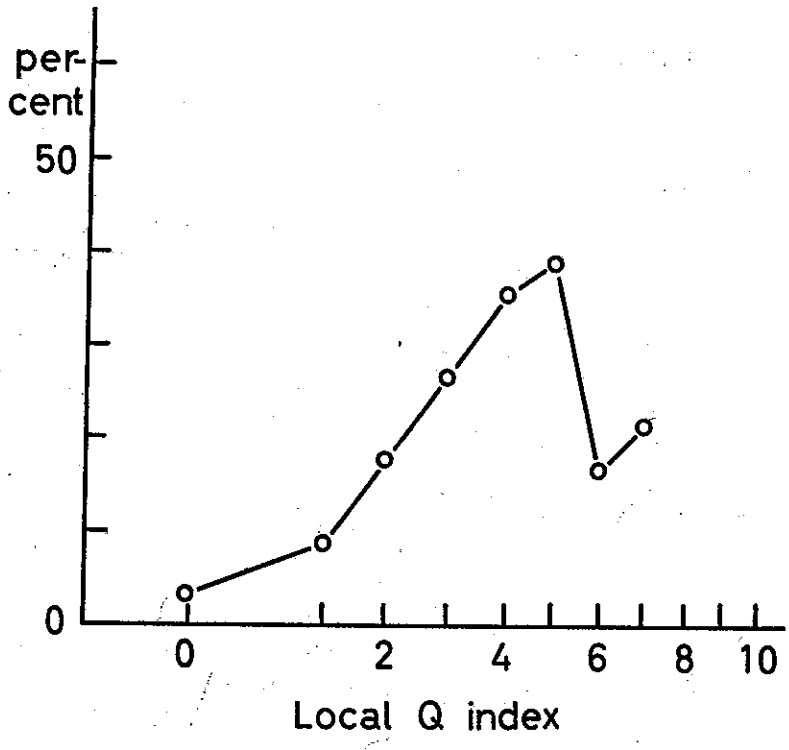

Fig. 15. Percentage occurrence of *Es* type *r* during different geomagnetical conditions at Halley Bay (After BELLCHAMBERS and PIGGOTT [18]).

a maximum in the occurrence of *Es* type *r* and a maximum of *fEs* is found at this station. Near midnight the storm current reaches its maximum intensity and is shifted towards its southernmost position. At this hour a clear maximum in the nocturnal variation of *fEs* is observed at all the Scandinavian stations south of the visual auroral zone, whereas a minimum occurs at Longyearbyen. Later in the night the sporadic *E* auroral zone moves northward, and a maximum in the *fEs* and in the occurrence of type *r* is observed at Tromsø at approximately 0300 MET, when the vertical component of the storm vector vanishes. During the morning hours, the electron density in the *Es* layer decreases gradually at all the Scandinavian stations, most rapidly at the southernmost stations. A short series of observations at Svalbard clearly demonstrates that the sporadic *E* auroral zone is shifted far to the north during the morning hours before it disappears. The Auroral Observatory in Tromsø operated a sweep frequency recorder at Bear Island (74.°5 N, 19.°3 E, 71° geom. lat.) during the autumn of 1959. A typical example of the diurnal variation of f_xEs for this station is shown in Fig. 16, together with the Tromsø-values. During the decay of the *Es* ionization at Tromsø the f_xEs increases at Bear Island up to 0245 MET when the zone of maximum passes the station.

The occurrence of the non-retardation type of *Es* seems to be non-affected by variations in the geomagnetic field. From a careful analysis there seems to be slight

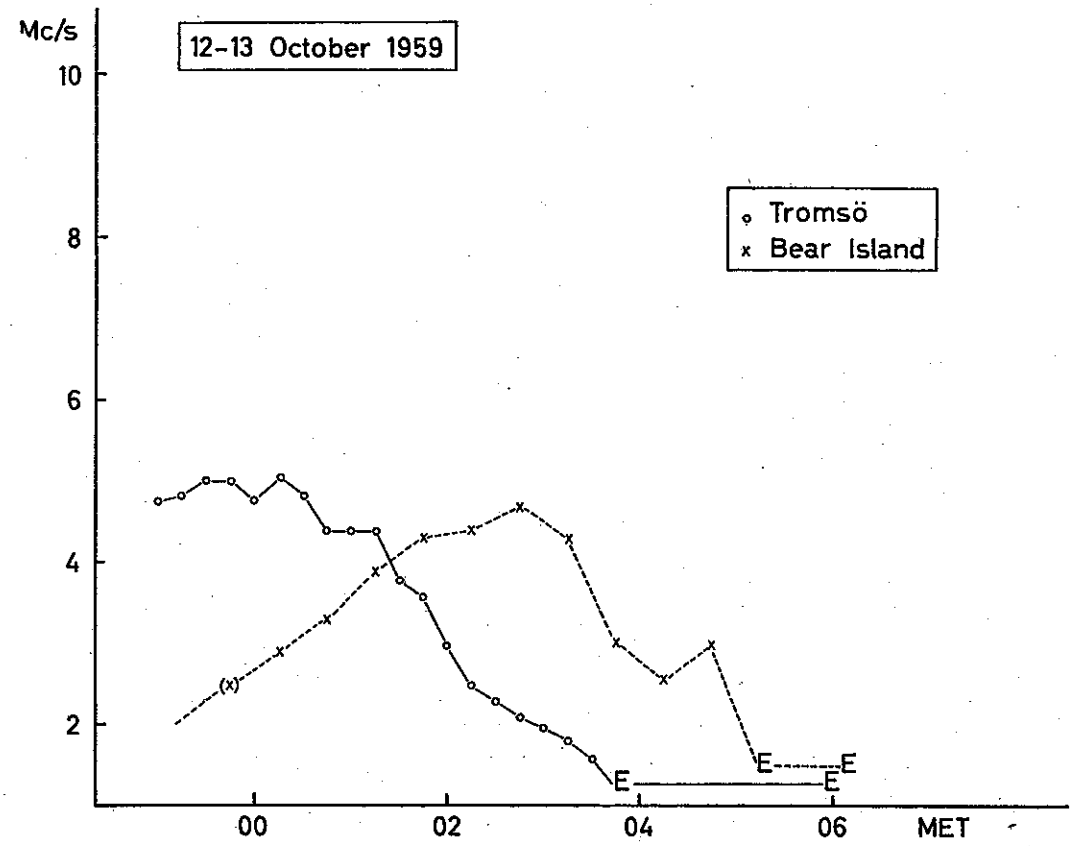

Fig. 16. Time variation of $f_r Es$ at Tromsø and Bear Island 12—13 October 1959.

evidence of more frequent occurrence of this type at the southern and northern border of the sporadic *E* auroral zone than in the centre of the zone. As, however, an unbiased statistical analysis of this point is very difficult, it will not be stressed. The scale of structure of the ionization in the *Es* region associated with the non-retardation type is somewhat less than 100 km. At sub-auroral zone stations a clear positive correlation between the $f_n Es$ and the local geomagnetic activity is found (BELLCHAMBERS and PIGGOTT [18]). In the auroral zone, however (Tromsø), the correlation is very low.

6.2 *Possible ionizing mechanisms.* A large number of theories has been put forward in order to explain the ionization in the *Es* region associated with polar magnetic storms and visual auroras. Although the theories differ in detail, they are all based on the assumption that high-energy electrons and protons are the main sources of ionization. Furthermore, that the high energies of the particles are directly or indirectly associated with solar phenomena.

This paper will not give the details of the different auroral theories. The early workers in this field (STØRMER [28], CHAPMAN and FERRARO [29], MARTYN [30] and ALFVÉN [31]) assumed that the "*auroral particles*" come directly from the sun, and their theories diverge mainly as far as the dynamics of the particles are concerned. During

recent years a number of auroral theories has been put forward, in which the ionizing particles are assumed to originate from areas in the vicinity of the earth where charged particles are trapped in the geomagnetic field (For a survey see PARKER [32]). These particles will obtain sufficient energy to penetrate into the auroral zone during solar storms when the geomagnetic field in the trapping region is distorted. The latter theories have been intensively studied by rocket and satellite measurements (VAN ALLEN [33] and MCILWAIN [14, 34]), and a clear connection between the auroral zone phenomena and variations in the outer *Van Allen belt* has been established.

The variations in the incoming particle stream associated with the meridional movements of the auroral zone during magnetic storms have been the subject of much speculation. It seems to be generally agreed that the equatorial shift of the auroral zone during geomagnetic storms is caused by an increase in the density and the energy of the solar stream. The information available on the geomagnetic field at a geocentric distance of 8—10 radii is very unsatisfactory. Furthermore, the distortion of the earth's magnetic field in the presence of a solar, corpuscular stream is still an unsolved problem. The correspondence between the variations in the auroral zone ionization and in the particle stream cannot therefore yet be studied quantitatively. Only a few details on the sources of ionization will be discussed.

Firstly, there seems to be an upper limit for the amount of ionization in the sporadic E auroral zone, characterized by the abrupt cut-off in the distribution function of f_rEs near 6 Mc sec^{-1}. This "cut-off" indicates that there is an upper limit for the incoming ionizing energy. For stationary conditions the relationship between the production q and the electron density n in the Es region is given by:

$$q = \alpha n^2 \tag{6.1}$$

The recombination coefficient α is during the night of the order 10^{-7} sec^{-1} (HOLT [35]). Thus the maximum plasma frequency observed in the sporadic E layer type r (6.3 Mc sec^{-1}) corresponds to a rate of production of $25 \cdot 10^3$ electrons cm^{-3} sec^{-1}, under stationary conditions. As the effective ionization potential is 40 eV, the energy support required for maintaining this rate of production is of the order 1 MeV cm^{-3} sec^{-1}.

The sporadic E layer type r has been ascribed to protons of extraterrestrial origin (SHAW [36]). The absorption of the energy of one single incoming proton, which is moving in a direction normal to the earth's surface, is shown in Figure 17, for different energy levels. Absorption parameters given by SEGRÉ [37], and atmosphere density parameters given by NEWELL [38] were used in the calculation of these curves. The illustration shows that protons of 100—250 keV energy may produce an ionospheric layer in the height range 100—200 km. For these energy levels the main part of the proton energy is absorbed between 100 and 125 km, and the maximum amount of energy absorbed is $9 \cdot 10^{-2}$ and $13{,}5 \cdot 10^{-2}$ eV per cm^3, for 100 and 200 keV energy protons, respectively.

Rocket measurements have shown that the flux density of protons with greater than 70 keV energy is $0{,}25 \cdot 10^6$ cm^{-2} sec^{-1} ster^{-1} above the atmosphere during hours

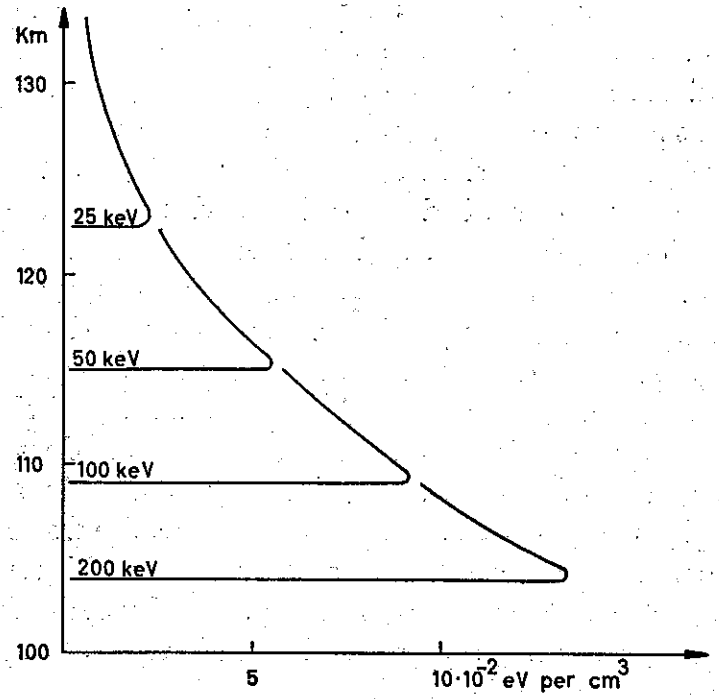

Fig. 17. Absorbed energy per incoming proton as function of height for different energy levels.

when a faint aurora is observed (McIlwain [14]). This flux density should, according to Fig. 17, produce an ionospheric layer with maximum plasma frequency equal to 2,5—3 Mc sec^{-1}. The flux density required for producing an ionospheric layer with a critical frequency of 6,3 Mc sec^{-1} is $(5 - 10) \cdot 10^6$ cm^{-2} sec^{-1}, if the proton energy is between 100 and 200 keV.

The ionization to be expected from a beam of mono-energetical protons is given in Fig. 18 for two different energy levels. In both cases the protons are assumed to move rectlinearly in a direction normal to the earth' surface. The flux density in the beam is so adjusted that the maximum electron density is the same for both layers. The layers have practically identical shapes, but a certain difference in height. The thickness of the layers is approximately 10—15 km. The sharp gradient near the lower boundary of the layer disappears if the energy spectrum of the incoming protons has a finite width.

It has been suggested (Shaw [36]) that the different *Es* types observed in the auroral zone are formed by different types of particles in the corpuscular stream. Thus, it is assumed that the *r* type is formed by protons originating from the radiation belts, whereas electrons of the same origin are the sources of the ionization of the *a* type. Shaw's model is based upon the assumption that the trapped particles are accelerated during solar storms by electrostatic waves set up in the upper atmosphere (Cole [39]).

The theory of Shaw [36] is interesting and attractive. An important conclusion may be drawn from this theory. As there most probably is charge equilibrium in the

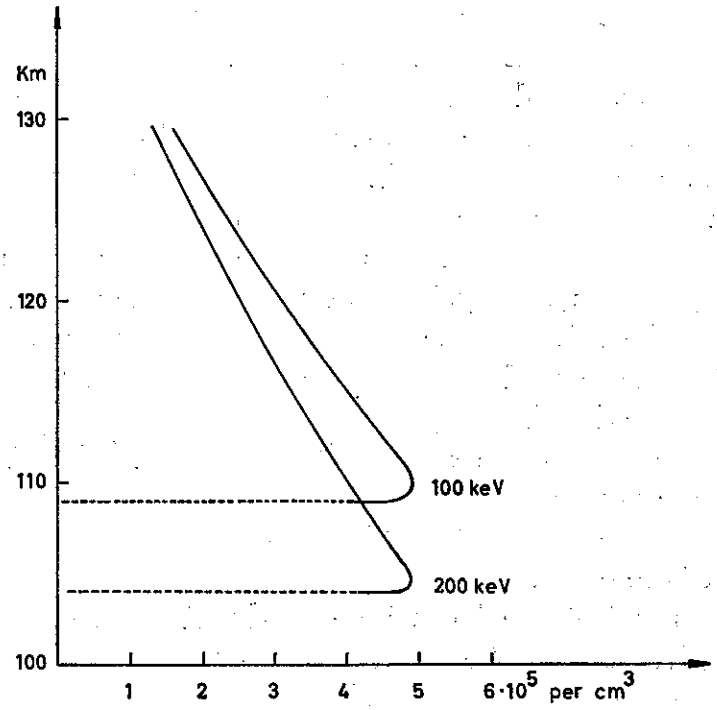

Fig. 18. Ionospheric layer with maximum plasma frequency equal to 6.3 Mc sec^{-1} formed by a stream of mono-energetic protons with energy 100 keV and 200 keV, respectively.

radiation belts, one whould expect the "scale of irregularity" in the incoming streams of protons and of electrons to be comparable. This implies that the mean "size" of the irregularities in the "*r*" layer should be of the same order of magnitude as the irregularities in the "*a*" layer.

From this argument and from the statistical study reported in the present document it seems improbable that the ionization mechanism suggested by SHAW is applicable for the "non-retardation" type of *Es* observed in the auroral zone.

The non-retardation type of *Es* is probably associated with ledges in the electron density profile or with thin layers of ionization. The zero correlation between magnetic activity and *Es* type *f* leads us to assume that these irregularities must be due to redistribution of existing ionization in the sporadic *E* auroral zone rather than formation of new electrons. The positive correlation between the top frequency of the non-retardation trace of *Es* and the magnetic activity at sub-auroral zone stations (BELLCHAMBERS and PIGGOTT [18]) may easily be explained by the enhanced electron "background" ionization in the sporadic *E* auroral zone during magnetic storms (Fig. 14).

The ionization associated with *Es* type *f* has to be left open for further studies. One particular point that seems worthy of study is to what extent the ionization associated with the non-retardation type of *Es* is related to the luminous and active auroras.

6.3 *Relationship between the sporadic E auroral zone and the polar magnetic storm.* The polar geomagnetic storm is normally ascribed to enhanced current density in the horizontal storm current, which is situated in the auroral ionosphere between 100 and 150 km altitude. This enhancement may be caused by increased conductivity in the current and/or an increased, external electric field at these heights.

The correspondence between the height of the storm current system and the sporadic E layer in the auroral zone indicates that the electrons in the layer are part of the current. In the previous sections it was shown that the sporadic E auroral zone moves north- and southwards in phase with the storm current system. In this section the relationship between the conductivity in the storm current and the electron density will be discussed in more detail.

The conductivity tensor C in the auroral zone is assumed to be a function of latitude Φ, altitude h and time t only:

$$C = C\,(a\Phi, h, t) \tag{6.2}$$

a being the radius of the earth.

The current density i in the ionosphere produced by a horizontal, meridional electric field $E\,(a\Phi, h, t)$ is therefore given by:

$$i\,(a\Phi, h, t) = C\,(a\Phi, h, t) \cdot E\,(a\Phi, h, t) \tag{6.3}$$

In the following the electric field E is assumed to be a function of time only:

$$i\,(a\Phi, h, t) = C\,(a\Phi, h, t)\; E\,(t) \tag{6.4}$$

The storm current in the auroral zone is quasi-zonal, and C is therefore equal to the "*Hall conductivity*". If the positive ions are assumed to be at rest, C is given by:

$$C\,(a\Phi, h, t) = \frac{n\,e^2\,\omega_e}{m_e\,(\nu_e^2 + \omega_e^2)} = K\,(h)\;n\,(a\Phi, h, t) \tag{6.5}$$

ω_e being the gyro frequency and ν_e the collision frequency for the electrons; e and m_e the charge and mass of the electron, respectively. n is the number density of free electrons.

The increment $\triangle i$ in the current density associated with geomagnetic storm conditions is given by:

$$\triangle i = (i_D - i_Q) = (C_D E_D - C_Q E_Q) \tag{6.6}$$

The indices D and Q refer to geomagnetically disturbed and quiet conditions, respectively.

The horizontal ($\triangle H$) and vertical ($\triangle Z$) components of the magnetic storm vector at a certain latitude $\Phi = \Phi_1$ are given by equations (6.7), in which the effect of induced earth currents has been neglected.

$$\begin{aligned} \triangle Z(t) &= \int\!\!\int \frac{a\,(\Phi - \Phi_1)\;\triangle i\,(a\Phi, h, t)}{(a\Phi - a\Phi_1)^2 + h^2}\; d\,(a\Phi)\; dh \\ \triangle H\,(t) &= \int\!\!\int \frac{h\,\triangle i\,(a\Phi, h, t)}{(a\Phi - a\Phi_1)^2 + h^2}\; d\,(a\Phi)\; dh \end{aligned} \tag{6.7}$$

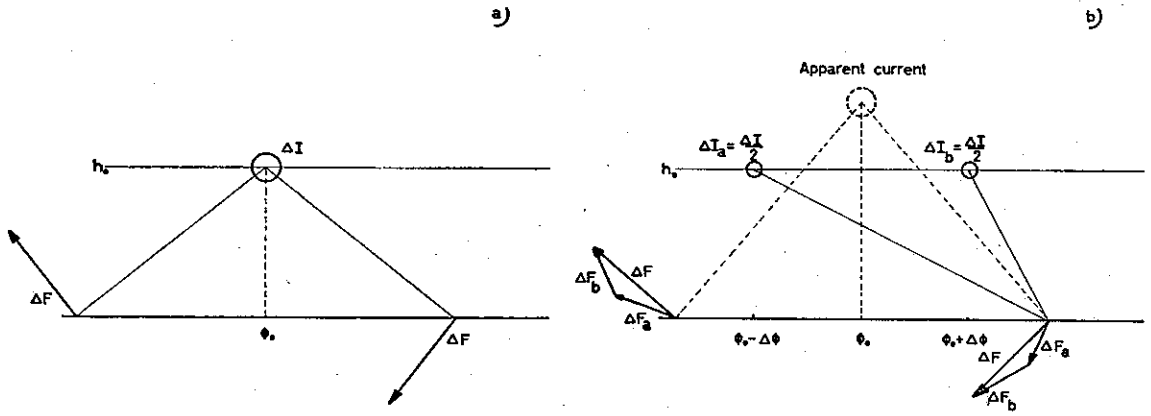

Fig. 19. Two different storm current models leading to different height of the apparent current.

The inclination angle α and the intensity $\triangle F$ of the storm vector is given by:

$$\tan \alpha = -\frac{\triangle Z}{\triangle H} \tag{6.8}$$

$$\triangle F = (\triangle H^2 + \triangle Z^2)^{1/2} \tag{6.9}$$

a. Assumed models of C $(a\Phi, h, t)$. Various models of the conductivity C as function of space and time have been put forth by different authors in order to explain the observed features of the geomagnetic storms. Most of the models differ, however, only slightly from the "linear current" model suggested by BIRKELAND [40]:

$$\begin{aligned} C(a\Phi, h, t) &= C(t) \text{ for } \Phi = \Phi_0 \text{ and } h = h_0 \\ C(a\Phi, h, t) &= O \text{ for } \Phi \neq \Phi_0 \text{ and } h \neq h_0 \end{aligned} \tag{6.10}$$

From simulatenous observations of *tan* α at different stations, BIRKELAND [40] deduced the parameters Φ_o and h_o for selected hours. Furthermore, from the storm intensity $\triangle F$ the total storm current $\triangle I = \int\int \triangle i \, d(a\Phi) \, dh$ was obtained. By this procedure BIRKELAND estimated h_o to be in the interval 160—1000 km.

The height of the current system seems in most cases to be seriously overestimated by BIRKELAND, as first pointed out by CHAPMAN [41]. The main reason for the overestimate was, according to Chapman, the neglection of the induced earth currents. From a harmonic analysis CHAPMAN argued that 30 to 40 per cent of the total storm vector is due to earth currents. A large number of workers has taken up this important problem. There appears, however, to be little agreement between the results obtained (HARANG [26], MCNISH [42], FLEMING et al [43] and VESTINE et al [44]), the percentage contribution from earth currents varying from 10 to 50. Most of these studies are based upon the "line-current" assumption.

Recently HEPPNER [45] has drawn attention to the fact that the "line-current" assumption itself will introduce an overestimate of the height h_0. This is visualized by the following simple example: Let a line current $\triangle I$ at Φ_0 (Fig. 19a) be replaced

by two parallel currents $\triangle I_a = \triangle I_b = \triangle I/2$ at the latitudes $(\Phi_0 + \triangle\Phi)$ and $(\Phi_0 - \triangle\Phi)$ (Fig. 19 b). After replacement, the inclination angle α is decreased, whereas the magnitude $\triangle F$ of the storm vector is relatively unchanged. The apparent height of the linear current is therefore greater in the latter example than in the former. It is evident that the importance of the earth current deduced from a model ionospheric current will be largely influenced by the choice of the spatial distribution of the conductivity in the ionosphere. Fig. 18 demonstrates that the linear-current assumption will normally lead to an over-estimate of the earth current.

If the results given in Figs. 13 and 14 are representative for the latitudinal variations of the electron density in the sporadic E layer and of the conductivity in the storm current system, there seems to be no doubt that the "line-current" assumption is seriously wrong. In the following the electron density profile in the *Es* layer is assumed to be parabolic, and the semi-thickness D of the layer is assumed to be constant in time and space. According to equation (6.5):

$$C(a\Phi, h, t) = K(h) \cdot \left(1 - \left(\frac{h - h_0}{D}\right)^2\right) \cdot n_m(a\Phi, t) \tag{6.11}$$

where h_0 is the level of maximum electron density n_m in the sporadic E layer ($n_m = 1/81 \cdot 10^{-6} (f_0 Es)^2$).

During heavily disturbed conditions $\triangle n = (n_D - n_Q) \gg 0$. If furthermore $E_D \approx E_Q$, equations (6.5) and (6.6) reduce to:

$$\triangle i \approx K(h) \cdot \triangle n \cdot E_D \tag{6.12}$$

As $K(h)$ is almost constant throughout the sporadic E layer, equation (6.7) reduces to:

$$\triangle Z = KE_D(t) \int\int \frac{a(\Phi - \Phi_1)\ \triangle n_m(a\Phi, t)}{a^2(\Phi - \Phi_1)^2 + h^2}\left(1 - \left(\frac{h - h_0}{D}\right)^2\right) \cdot d(a\Phi)\, dh \tag{6.13}$$

$$\triangle H = KE_D(t) \int\int \frac{h\, \triangle n_m(a\Phi, t)}{a^2(\Phi - \Phi_1)^2 + h^2}\left(1 - \left(\frac{h - h_0}{D}\right)^2\right) \cdot d(a\Phi)\, dh \tag{6.14}$$

The inclination angle α has been deduced by equations (6.13), (6.14) and (6.9) for Tromsø ($\Phi_1 = 67°$ geom. lat.) for a number of hours. In the calculations the parameters h_0 and D were assumed to be 110 km and 10 km, respectively. The deduced values of α have been compared with the observed values, and there is a remarkable consistency between the values. This result seems to indicate that the contribution from the induced earth currents to the storm vector is of minor importance. As, however, the latitude distribution of $\triangle n_m$ is very uncertain, especially north of 67° geom. lat., the significance of this result is somewhat doubtful. In this paper only the values of *tan* α deduced for the mean, meridional "cross-sections" given in Fig. 14 are presented (Table 4).

Although the numerical results reported in this section are somewhat dubious, due to lack of observations, the close correspondence between the electron density in the sporadic E layers and the current density in the storm current is well established. In

Table 4. Theoretical and observed values of *tan α*.

	Observed	Deduced
group 3a	− 0.9	− 0.93
3b	0	+ 0.07
3c	+ (0.60 − 0.63)	+ 0.61

order to study the variations in the electric field $E(t)$ and the induced earth currents it seems to be more fruitful to assume a model of the conductivity as given in equation (6.11) rather than that given in equation (6.10). In order to deduce the latitude distribution of $\triangle n_m$ with sufficient accuracy it is, however, important to use a much denser network of ionosonde stations than that used during this study.

Acknowledgements. The author would like to express his gratitude to all his assistants during the study, particulary to Mr. R. LARSEN and Mr. L. LORNTZSEN at the Auroral Observatory of Tromsø who took part in the observations, and to Mr. N. O. NIELSEN, Mrs. I. J. TORGERSEN and Miss J. ANDERSEN who have done the onerous job of data reduction.

The gratitude is extended to the author's colleagues at the Norwegian Defence Research Establishment for stimulating discussion and suggestions, especially to dr. B. LANDMARK and to professor L. HARANG.

Fig. 15 is reproduced with the permission of W. H. BELLCHAMBERS.

The work was supported by the EO—ARDC under contract *AF 61(052)—228.*

REFERENCES

1. SMITH, E. K.: *N. B. S. Circular* 582, Nat. Bur. Stand. (1957).
2. CORONITI, S. C., and R. PENNDORF: *Science Report* No. 1, AVCO (1958). *J. Geophys. Res.*, **63**, 789 (1958).
3. SMITH, E. K., and J. A. Thomas: *N. B. S. Report* 5564, Nat. Bur. Stand. (1958).
4. RAWER, K.: *Geofis. pura e appl.*, **32**, 170 (1955).
5. BECKER, W.: *AGARDograph* No. 34 (1958) and private communication.
6. MEEK, J. H.: *URSI Spring Meeting*, Washington D. C. (1947).
7. JACKSON, J. E.: Private communication.
8. OLESEN, J. K., and J. RYBNER: *AGARDograph*, No. 34 (1958).
9. BESPROZVANNAYA, A. S., and V. A. LOVCOVA: *Tr. Arct. Res. Inst.* USSR (1956) (Engl. transl. by E. R. Hope).
10. MÆHLUM, B.: *NDRE Report* No. 29, Norwegian Defence Res. Est. (1958).
11. KNECHT, R. W.: *J. Geophys. Res.*, **61**, 59 (1956).
12. OMHOLT, A.: *J. Atmosph. Terr. Phys.*, **7**, 73 (1955).
13. LEADABRAND, R. L., L. DOLPHIN, and A. M. PETERSON: *Final Rep. Contract* AF 30(602)—1462, Stanford Res. Inst. (1957).
14. MCILWAIN, C. E.: SUI—59—29, *State Univ. Iowa* (1959).
15. URSI/AGI Committee: *Second Rep. Spec. Comm. on World Wide Ionosph. Soundings*, URSI (1957).

16. WRIGHT, J. W., and R. W. KNECHT: *Atlas of Ionograms*, CRPL, Nat. Bur. Stand. (1957).
17. LINDQUIST, R.: *Ark. Geofys.*, **1**, No. 11 (1951).
18. BELLCHAMBERS, W. H., and W. R. PIGGOTT: *Proc. Roy. Soc.*, **A256**, 200 (1960).
19. NAISMITH, R., and R. BAILEY: *Proc. Inst. Electr. Engrs.*, III, **98**, 11 (1951).
20. BULLOUGH, K., and T. R. KAISER: *J. Atmosph. Terr. Phys.*, **5**, 189 (1954).
21. NICHOLS, B.: *Proc. Inst. Radio Engrs.*, **47**, 245 (1959).
22. MATSUSHITA, S.: *J. Atmosph. Terr. Phys.*, **15**, 68 (1959).
23. HARANG, L., O. KROGNESS, and E. TØNSBERG: *Publ. Norske Inst. Kosmisk Fysikk*, **2** (1933).
24. VESTINE, E. H.: *Terr. Mag.*, **49**, 77 (1944).
25. NAGATA, T.: *J. Geophys. Res.*, **55**, 127 (1950).
26. HARANG, L.: *Geofys. Publ.*, **16**, No. 12 (1946).
27. CHAPMAN, S., and J. BARTELS: *Geomagnetism*, Oxford (1940).
28. STØRMER, F. C. M.: *The Polar Aurora*, Oxford (1955).
29. CHAPMAN, S., and V. C. A. FERRARO: *Terr. Mag.*, **36**, 77 and 171 (1931) and **37**, 147 (1932).
30. MARTYN, D. F.: *Nature*, **167**, 92 (1951).
31. ALFVEN, H.: *Kungl. Svenska Vetenskapsakad. Handl.*, **18**, 3 (1939) and 9 (1940).
32. PARKER, E. N.: *Proc. Inst. Radio. Engrs.*, **47**, 239 (1959).
33. VAN ALLEN, J. A.: *Bibliography given in Proc. Roy. Soc.*, **A253**, 525 (1959).
34. MCILWAIN, C. E.: *J. Geophys. Res.*, **65**, 2727 (1960).
35. HOLT, O.: Private communication.
36. SHAW, J. E.: *Planet. Space Sci.*, **2**, 49 (1959).
37. SEGRE, E.: *Experimental nuclear physics*, **1**, New York (1953).
38. NEWELL, H. E.: *High altitude rocket research*, New York (1953).
39. COLE, K. D.: *Nature*, **183**, 738 (1959).
40. BIRKELAND, K.: *Videnskabsselskabets Skrifter*, I. Matematisk-Naturvidenskabelig Klasse, 1 (1901).
41. CHAPMAN, S.: *Terr. Mag.*, **40**, 349 (1935).
42. MCNISH, *A.* G.: *Terr. Mag.* **43**, 67 (1938).
43. FLEMING, J. A., A. G. MCNISH, L. VEGARD, et al: *Terrestrial Magnetism and Electricity*, New York (1949).
44. VESTINE, E. H., L. LAPORT, I. LANGE, and W. E. SCOTT: *The Geomagnetic Field, Carnegie Inst. Washington*, Publ. 580 (1947).
45. HEPPNER, J. P.: *Def. Res. Board*, Canada, Report DR 135, (1958).

INNHOLD

		Side
No. 1.	**Bernt Mæhlum.** The sporadic *E* auroral zone	1—32
« 2.	**Bernt Mæhlum.** Small scale structure and drift in the sporadic *E* layer as observed in the auroral zone.....	1—19
« 3.	**L. Harang** and **K. Malmjord.** Determination of drift movements of the ionosphere at high latitudes from radio star scintillations....	1—12
« 4.	**Eyvind Riis.** The stability of Couette-flow in non-stratified and stratified viscous fluids.....	1—37
« 5.	**E. Frogner.** Temperature changes on a large scale in the arctic winter stratosphere and their probable effects on the tropospheric circulation.....	1—83
« 6.	**Odd H. Sælen.** Studies in the Norwegian Atlantic current. Part II: Investigations during the years 1954–59 in an area west of Stad....	1—82

Avhandlinger som ønskes opptatt i «Geofysiske Publikasjoner», må fremlegges i Videnskaps-Akademiet av et sakkyndig medlem.

Vol. XX.

No. 1. B. J. Birkeland: Homogenisierung der Temperaturreihe Greenwich 1763—1840. 1957.
» 2. Enok Palm: On Reynolds stress, turbulent diffusion and the velocity profile in stratified fluid. 1958.
» 3. Enok Palm: Two-dimensional and three-dimensional mountain waves. 1958.
» 4. L. Vegard: Recent progress relating to the study of aurorae and kindred phenomena. 1958.
» 5. Leiv Harang: Heigth distribution of the red auroral line in polar aurorae. 1958.
» 6. Bernt Mæhlum: The diurnal- and sunspot-cycle variation of the layers *E*, *F*1 and *F*2 of the ionosphere as observed in Norway during the period 1932—1956. 1958.
» 7. Jonas Ekman Fjeldstad: Ocean current as an initial problem. 1958.
» 8. Olav Holt and Bjørn Landmark: Some statistical properties of the signal fine structure in ionospheric scatter propagation. 1958.
» 9. L. Vegard, S. Berger, and A. Nundal: Results of auroral observations at Tromsø and Oslo from the four winters 1953—54 to 1956—57. 1958.
» 10. Eigil Hesstvedt: Mother of pearl clouds in Norway 1959.
» 11. A. Omholt: Studies on the excitation of aurora borealis. I. The hydrogen lines. 1959.
» 12. G. Kvifte: Nightglow observations at Ås during the I. G. Y. 1959.
» 13. Odd H. Sælen: Studies in the Norwegian Atlantic current. Part I: The Sognefjord section. 1959.

Vol. XXI.

No. 1. A. Omholt: Studies on the excitation of aurora borealis II. The forbidden oxygen lines. 1959.
» 2. Tor Hagfors: Investigation of the scattering of radio waves at metric wavelengths in the lower ionosphere. 1959.
» 3. Håkon Mosby: Deep water in the Norwegian Sea. 1959.
» 4. Søren H. H. Larsen: On the scattering of ultraviolet solar radiation in the atmosphere with the ozone absorption considered. 1959.
» 5. Søren H. H. Larsen: Measurements of atmospheric ozone at Spitsbergen (78°N) and Tromsø (70°N) during the winter season. 1959.
» 6. Enok Palm and Arne Foldvik: Contribution to the theory of two-dimensional mountain waves 1960.
» 7. Kaare Pedersen and Marius Todsen: Some measurements of the micro-structure of fog and stratus-clouds in the Oslo area. 1960.
» 8. Kaare Pedersen: An experiment in numerical prediction of the 500 mb wind field. 1960.
» 9. Eigil Hesstvedt: On the physics of mother of pearl clouds. 1960.

Vol. XXII.

No. 1. L. Harang and K. Malmjord: Drift measurements of the E-lager at Kjeller and Tromsø during the international geophysical year 1957—58. 1960.
» 2. Leiv Harang and Anders Omholt: Luminosity curves of high aurorae. 1960.
» 3. Arnt Eliassen and Enok Palm: On the transfer of energy in stationary mountain waves. 1961.
» 4. Yngvar Gotaas: Mother of pearl clouds over Southern Norway, February 21, 1959. 1961.
» 5. H. Økland: An experiment in numeral integration of the barotropic equation by a quasi-Lagrangian method. 1962.
» 6. L. Vegard: Auroral investigations during the winter seasons 1957/58—1959/60 and their bearing on solar terrestrial relationships. 1961.
» 7. Gunnvald Bøyum: A study of evaporation and heat exchange between the sea surface and the atmosphere. 1962.

Vol. XXIII.

No. 1. Bernt Mæhlum: The sporadic E auroral zone. 1962.
» 2. Bernt Mæhlum: Small scale structure and drift in the sporadic E layer as observed in the auroral zone. 1962.
» 3. L. Harang and K. Malmjord: Determination of drift movements of the ionosphere at high latitudes from radio star scintillations. 1962.
» 4. Eyvind Riis: The stability of Couette-flow in non-stratified and stratified viscous fluids. 1962.
» 5. E. Frogner: Temperature changes on a large scale in the arctic winter stratosphere and their probable effects on the tropospheric circulation. 1962.

A.s John Griegs Boktrykkeri